This Page Is Inserted by IFW Operations
and is not a part of the Official Record

BEST AVAILABLE IMAGES

Defective images within this document are accurate representations of the original documents submitted by the applicant.

Defects in the images may include (but are not limited to):

- BLACK BORDERS
- TEXT CUT OFF AT TOP, BOTTOM OR SIDES
- FADED TEXT
- ILLEGIBLE TEXT
- SKEWED/SLANTED IMAGES
- COLORED PHOTOS
- BLACK OR VERY BLACK AND WHITE DARK PHOTOS
- GRAY SCALE DOCUMENTS

IMAGES ARE BEST AVAILABLE COPY.

As rescanning documents *will not* correct images, please do not report the images to the Image Problem Mailbox.

(12) INTERNATIONAL APPLICATION PUBLISHED UNDER THE PATENT COOPERATION TREATY (PCT)

(19) World Intellectual Property Organization
International Bureau

(43) International Publication Date
2 May 2002 (02.05.2002)

PCT

(10) International Publication Number
WO 02/35214 A1

(51) International Patent Classification[7]: G01N 21/77

(21) International Application Number: PCT/EP01/12366

(22) International Filing Date: 25 October 2001 (25.10.2001)

(25) Filing Language: English

(26) Publication Language: English

(30) Priority Data:
0026346.7 27 October 2000 (27.10.2000) GB

(71) Applicant *(for all designated States except US)*: **RISØ NATIONAL LABORATORY** [DK/DK]; Frederiksborgvej 399, DK-4000 Roskilde (DK).

(72) Inventors; and
(75) Inventors/Applicants *(for US only)*: **HORVÁTH, Róbert** [HU/HU]; Warga L. 16/1, H-3200Gyöngyös (HU). **PEDERSEN, Henrik, Chresten** [DK/DK]; Stenkrogen 28, DK-4040 Jyllinge (DK). **LINDVOLD, Lars, René** [DK/DK]; Kornager 210, DK-2980 Kokkedal (DK). **LARSEN, Niels, Bent** [DK/DK]; Borghaven 34 B 1, DK-2500 Valby (DK).

(74) Agent: **SMART, Peter, J.**; W.H. Beck, Greener & Co., 7 Stone Buildings, Lincoln's Inn, London WC2A 3SZ (GB).

(81) Designated States *(national)*: AE, AG, AL, AM, AT, AU, AZ, BA, BB, BG, BR, BY, BZ, CA, CH, CN, CO, CR, CU, CZ, DE, DK, DM, DZ, EC, EE, ES, FI, GB, GD, GE, GH, GM, HR, HU, ID, IL, IN, IS, JP, KE, KG, KP, KR, KZ, LC, LK, LR, LS, LT, LU, LV, MA, MD, MG, MK, MN, MW, MX, MZ, NO, NZ, PH, PL, PT, RO, RU, SD, SE, SG, SI, SK, SL, TJ, TM, TR, TT, TZ, UA, UG, US, UZ, VN, YU, ZA, ZW.

(84) Designated States *(regional)*: ARIPO patent (GH, GM, KE, LS, MW, MZ, SD, SL, SZ, TZ, UG, ZW), Eurasian patent (AM, AZ, BY, KG, KZ, MD, RU, TJ, TM), European patent (AT, BE, CH, CY, DE, DK, ES, FI, FR, GB, GR, IE, IT, LU, MC, NL, PT, SE, TR), OAPI patent (BF, BJ, CF, CG, CI, CM, GA, GN, GQ, GW, ML, MR, NE, SN, TD, TG).

Published:
— *with international search report*
— *before the expiration of the time limit for amending the claims and to be republished in the event of receipt of amendments*

For two-letter codes and other abbreviations, refer to the "Guidance Notes on Codes and Abbreviations" appearing at the beginning of each regular issue of the PCT Gazette.

(54) Title: REVERSE SYMMETRY WAVEGUIDE FOR OPTICAL BIOSENSING

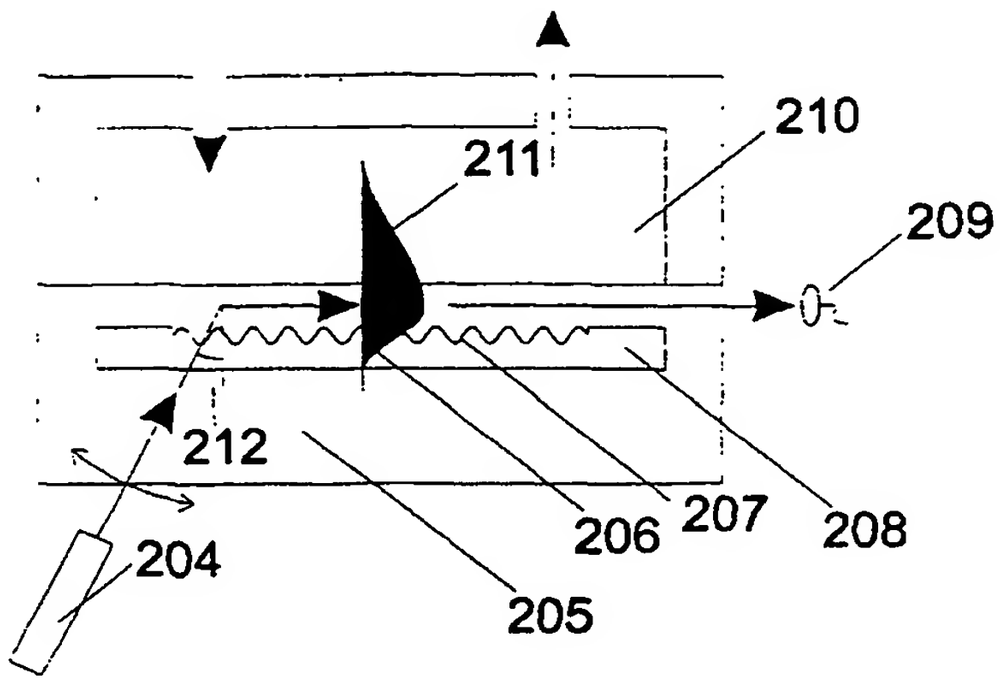

(57) Abstract: An optical waveguide sensor comprises a substrate material (208), having a refractive index n_s, typically an air containing groove (208) in the surface of a polymer structural substrate (205), an optical waveguide film (207) on the substrate material having a refractive index n_F, and a cover material (210) over the waveguide having a refractive index n_c, a light source (204) optically coupled to said waveguide, and a detector (209) for detecting evanescent wave interaction between said light and said cover material, wherein $n_F > n_S >$ and $n_F > n_C$ and $n_C > n_S$, and $n_C < 1.45$. The low refractive index of the substrate enables sensing of material in the cover further from the waveguide than would conventionally be possible.

WO 02/35214 A1

Reverse Symmetry Waveguide For Optical Biosensing

Background of the invention

This invention relates to the field of optical waveguide sensors. Methods are disclosed for the fabrication and application of optical biosensors based on evanescent wave sensing in planar waveguides, for chemical, biochemical, or biological analysis. Biological analysis includes, but is not restricted to, detection or intracellular analysis of prokaryotes and eukaryotes as well as detection or analysis of secretions from such organisms.

The essential part of a generic optical waveguide sensor is shown in Fig. 1. The sensor consists of a thin (about 200 - 500 nm thickness) waveguiding film (101) having on one side a solid substrate medium (102) and on the other side a cover medium (100). The cover medium is a (typically aqueous) sample to be analysed. The refractive indices of the three media are chosen so that the refractive index of the film is larger than those of the two surrounding media. In this case, light is guided by total internal reflection from one end of the film to the other, without being able to escape from the film.

Despite the fact that light cannot propagate into the surrounding media, the transversal profile of the guided light mode (108) still extends into both the substrate and the cover. These two parts of the light mode are referred to as the mode's evanescent tails, i.e. substrate tail (104) and cover tail (103), as their field amplitudes decay exponentially away from the film.

In terms of sensing, the cover tail is the most important part of the light mode, as this tail is capable of sensing changes in either the refractive index, the absorbance, or the fluorescence of the cover medium. In a biosensor the changes in these three parameters occur as a result of chemical, biochemical, or biological reactions occurring in an aqueous cover medium or between a component of the cover medium and the waveguiding material, or physical interactions between the waveguiding material and a component in the cover medium. Hence, by various techniques, some of which involve measuring changes in the properties of the guided light, such as speed or wavelength spectrum, it is possible to monitor the desired chemical, biochemical, or biological reactions taking place in the cover medium or at the film-cover interface or in the film. The cover tail may also transfer energy from the guided light to predefined regions of the cover medium and thereby excite or otherwise affect changes to the cover medium or parts thereof that may be used for analysis purposes, for example fluorescence.

In known optical biosensors, based on evanescent wave sensing in planar metaloxide waveguides, there is a fundamental limit to the length of the cover tail (probing or penetration depth) into the cover medium, which is no more than 100 - 200 nm (cf. K. Tiefenthaler and W. Lukosz, Journal of the Optical Society of America B, 6 (1989) 209-220; W. Lukosz, Sensors and Actuators B, 29 (1995) 37-50; R. E. Kunz, Sensors and Actuators B, 38-39 (1997) 13-28). Such sensors exhibit very high sensitivities in terms of measuring changes occurring within this short distance from the film surface.

However, during the last five years, people have started using the optical waveguide sensor in new areas of biological research, namely for the detection of reactions involving larger substances. This includes the detection and monitoring of adhesion, spreading, and growth of living cells (eukaryotes) (J.J. Ramsden et al., Biotechnology and Bioengineering, 43 (1994) 939-945; J. J. Ramsden et al., Cytometry, 19 (1995) 97-102; A. M. Hutchinson, Molecular Biotechnology, 3 (1995) 47-54; L. Ruiz, Journal of Biomaterial Science Polymer Edition, 10 (1999) 931-955; S. Hirmo et al., Analytical Biochemistry, 257 (1998) 63-66) and detecting the adhesion of bacteria (prokariotes) to a proteinlayer (S. Hirmo, Journal of Microbiological Methods, 37 (1999) 177-182). Along this line, one could further think of the long cover tail's in vivo monitoring of intracellular reactions as well as the detection of certain prokaryotes' presence, adhesion, growth, interaction with cells and extracellular secretions in, for example, biofilms.

In this case, the penetration depth of the cover tail becomes a very important parameter because these substances assume sizes of 0.1 - 5 µm (prokaryotes) and 10 - 100 µm (eukaryotes), which are much larger than the cover penetration depth of a state of the art waveguide sensor. Thus, the short cover tail only senses the very nearest part of the large particles giving rise to a rather weak response (R. Kurrat, Ph.D. Dissertation #12891, ETH Zürich, 1998). Therefore, a new sensor type with a larger penetration depth into the cover is needed for this purpose. Moreover, it would be preferable, if the cover penetration depth could be controlled in an unlimited manner in the manufacturing of the

waveguide, to be able to fabricate waveguide modules for specific types of measurement.

In the present invention, we present a new sensor type, based on a so-called reverse symmetry design, in which the penetration depth of the cover tail may be controlled up to a depth of, in principle, infinity.

K. Tiefenthaler and W. Lukosz, Journal of the Optical Society of America B, 6 (1989) 209-220 in a theoretical discussion of the physics in waveguide sensors discusses the theoretical case of having $n_c > n_s$, where n_c is the refractive index of the cover and n_s is the refractive index of the substrate. The authors calculate the properties of such a system in which the cover medium is an organic solvent (n_c = 1.50), the substrate being glass (n_s = 1.47) and show that the penetration depth in the cover material will increase as the waveguiding film thickness decreases. No actual sensor having a measurand is described.

This theoretical behaviour is noted also in O. Parriaux et al, Sensors and Actuators B 29, 1995, pp 289-292, although without reference to any materials. It is said that the concept is not relevant to the grating coupled evanescent wave type of immunosensor.

The present invention provides in a first aspect an optical waveguide sensor comprising a substrate material having a refractive index n_s, an optical waveguide film on the substrate material having a refractive index n_F, and a cover material over the waveguide having a refractive index n_c, a light source optically coupled to said waveguide, and a detector for detecting evanescent wave interaction between

said light and said cover material, wherein $n_F > n_s$ and $n_F > n_c$ and $n_c > n_s$ and $n_c < 1.45$, more preferably $n_c < 1.4$.

The main idea relies on reversing the symmetry of the substrate-film-cover refractive indices, still so that the film refractive index is the largest, but, in addition, so that the substrate refractive index is less than the cover index. This is opposed to the conventional chemical or biological waveguide sensor, where the substrate is usually glass, silica, or a polymer, which all have a refractive index between, say, 1.4 - 1.6, hence, larger than that of water (1.333). The opportunity of reversing the symmetry has previously been overlooked, probably because of the absence of a convenient substrate material with a refractive index less than 1.333.

In the present invention, however, we have appreciated that it is possible in a waveguided sensor to arrange that the value of n_c is more than that of n_s, for instance by using air or an air containing material as the substrate, resulting in a sufficiently low substrate refractive index.

Preferably, in a sensor of the invention $n_s < 1.3$.

Preferably, the cover material is an aqueous medium. This especially lends itself to use in a wide range of chemical and biochemical sensing applications. Biochemical systems especially are often only viable in water, often requiring near physiological conditions.

Preferably, the substrate material is a gas or a gas containing material. The term 'substrate material' is used here in the sense usual and conventional in defining waveguiding sensors to mean the material bordering the waveguide on the opposite side to the cover material. Where

the substrate is a gas, it does not of course have the function of physically supporting the waveguide film.

The substrate material is preferably air or an air containing material. Air containing materials include solids having pores or micro-pores containing air. Similar pore containing materials containing other gases may of course be used.

However, we have also devised a structure in which substrate is air and is contained in an air space defined by an air groove in a solid material which is in physical contact with the waveguiding film and which has a depth larger than the air-substrate penetration depth of the light.

The substrate surface may incorporate nano-structures being less than a wavelength of said light in size, thus providing gas spaces adjacent the waveguide film.

The sensor may include a housing containing said cover material in contact with said waveguide, said housing having an inlet for the introduction of a sample for sensing. Said housing may form a flow cell through which a said sample constituting said cover material can be flowed in use.

Preferably, the waveguide is constituted by a polymer film. This may be of a light-cured polymer. Suitable polymers include polystyrene, polycarbonate, polymethacrylate (PMMA), and other optical polymers, preferably having low absorption. Suitably, the waveguide thickness is 200 to 500 nm. Coupling grating modulation depth may be 3 to 60 nm, e.g. 3 to 30 nm. The waveguides preferably are monomodal.

Light from the light source may coupled into and/or out from the waveguide in various ways such as via coupling gratings incorporated in the waveguide, through an optical

prism or through end facets of the waveguide. Light may be guided to and/or from the coupling elements through an optical fibre. Where gratings are used, the grating period may be from 200 to 1000 nm. Preferably, each grating has a single periodicity and if both incoupling and outcoupling gratings are used they are preferably of different periodicities. However, one may use a grating with broad spectrum of Λ (grating spacing), a so-called chirped grating, illuminated with a monochromatic source so that the position on the grating (x), which represents a certain value of $\Lambda(x)$, where light is coupled in provides a value of N.

The light from the light source which is incident on the waveguide film may be a collimated light beam or a focused light beam and for this purpose the sensor may include a collimator or a focusing system or a defocusing system interposed between the light source and the waveguide film.

The light source may be a laser or a non-monochromatic light source. Where said light source is non-monochromatic, a monochromator may be interposed between the light source and said waveguiding film. However, rather than using a monochromator it may be preferable to illuminate the coupling grating with a broad range of wavelengths. This removes the need to scan the source over angles to find the correct coupling angle, because the grating will select that wavelength for which the coupling angle used is appropriate and the coupled wavelength will serve as a measure of the effective refractive index N (see Equation 4 below). Dye lasers gas lasers, solid state lasers and semi-conductor diode lasers may all be used.

Suitable detectors include photodiodes, photocells, photomultipliers, CCD cameras and detector arrays such as CCD rows and 2-D CCD arrays, or photographic film cameras. The light output may be passed through a wavelength separating device such as a filter, prism, monochromator or diffraction grating prior to detection.

Detection may involve splitting a light input to the sensor and passing the light along two light paths, one serving as a reference and the other passing through a sensor according to the investigation in which a suitable measurand or analyte is present, followed by recombining of the light beams and the detection of beating between them. Such a system is described for instance in US 4950074.

Alternatively, to provide an internal reference, light may be propagated through the waveguide as two orthogonal, coherent, polarised modes, one of which preferentially interacts with the sample, and the phase difference induced between the modes may be detected as a polarisation shift as described in more detail in US5120131.

The waveguide film may be incorporated into the cavity of a laser to amplify the effect of the interaction with the measurand by effectively multiplying the optical path length over which it occurs.

The effective path length can also be increased as in US 5081012 in which the input and output coupling gratings are side-by-side and a reflecting grating is positioned in front of them.

Sensors of the invention may be arranged in a one dimensional or two dimensional array. The invention therefore includes an array of two or more sensors as

described above. Preferably, at least one of the sensors in the array is for use as reference sensor. In use, when the array is used for detecting or quantitating a substance in a sample, the reference sensor may be not exposed to the substance or may be unresponsive to the substance.

In such an array of sensors different sensors may have been chemically designed to react with different substances. This may be by virtue of placing specific binding partners for different materials in said array locations. These may be antibody fragments, antibody binding ligands, micro-organisms or cells bearing proteins recognisable by antibodies in the cover material, or chemical entities. Such materials may also be placed on the waveguide film in embodiments in which there is only one sensor rather than an array.

Such entities may be applied, especially at an array of sites, by for instance methods discussed in US 6078705, including ink jet type printing, the use of a flow cell, stamping materials on to the waveguide surface or other printing methods. An adhesion promoting layer may be applied first to the waveguide film. Microbeads may be applied to the waveguide surface to increase its effective surface area.

In such an array, there may be one or more detectors shared in common between one or more of the sensors of the array.

Array systems are described in US 5738825 and such arrays may readily be adapted to be constructed according to the principles of this invention.

Sensors according to the invention may be used in numerous assay formats including competition assays and

sandwich assay as generally known in the art. In a typical sandwich assay, a captive reagent such as an antibody on the waveguide surface may be used to capture a measurand such as a cell and a recognition agent such as a labelled antibody, for instance a fluorescence labelled antibody, may then be bound to the captured measurand.

The analyte in an assay performed using the sensor of the invention may be a constituent in an aqueous solution or suspension which may optionally include buffers and/or additional solvents.

The invention includes a method for sensing evanescent wave interaction between light and a sample material, comprising introducing said sample material as or into said cover material in a sensor as described above, and detecting said interaction using said detector of the sensor.

In such a method, said sample may produce an alteration in said cover material at least 200 nm away, e.g. at least 500 nm away, from said waveguide, which alteration in said cover material is detected as a change in said evanescent wave interaction between said light and said cover material.

The sample may include micro-organisms or biological cells whose interaction with each other or with the waveguide surface changes the optical properties of said evanescent wave and the optical properties of the waveguided light.

In a further aspect, the invention includes a method of fabricating an optical waveguide sensor unit, comprising:

a) forming an optical coupling grating master by forming a layer of photoresist polymer on a surface, exposing said photoresist polymer to interfering monochromatic light

beams such that interference fringes formed by said light beams expose the photoresist such that upon development the photoresist forms an optical grating pattern, developing said photoresist to form said optical grating pattern as said optical grating master,

b) casting a negative polymer impression of said master by applying a settable polymer thereto, setting said polymer and removing said polymer from said master,

c) impressing said negative polymer impression of the optical grating pattern into a light-curable polymer film supported by a temporary support substrate and partially curing the light-curable polymer followed by removal of said negative imprint of the optical grating leaving a positive replica of said optical grating pattern in the partially cured polymer film,

d) forming a master of a shallow groove by forming a layer of photoresist polymer on a surface, exposing said photoresist polymer to light such that said light exposes the photoresist in a desired groove pattern such that upon development the photoresist forms walls bordering a groove of which said surface forms a base, developing said photoresist to form said groove pattern as said groove master,

e) casting a negative impression of said groove master by applying a settable polymer thereto, setting said

polymer and removing said polymer from said groove master,

f) casting a light-curable polymer onto said negative impression of the groove master and partially curing the same followed by removal of said partially cured polymer bearing a groove which is a positive replica of said groove master,

g) uniting said positive replica of the groove master and the positive replica of the optical grating pattern such that together they form a conduit having said film incorporating said optical grating pattern spanning said groove and bonding the two positive replicas together by completing the cure of said partially cured polymer, and

h) removing said temporary support substrate from the polymer film incorporating said optical grating pattern.

Preferably, each negative impression is formed in a heat curable silicone rubber. Said temporary support substrate is preferably formed of a soluble polymer and is removed by being dissolved in an appropriate solvent.

A particular virtue of this method is that the masters of the optical grating pattern and the groove may be used repeatedly in steps (b) and (e) of said method.

The invention in its preferred aspects will be further described and illustrated with reference to the accompanying drawings, in which:-

Figure 1 is a schematic side view of a generic grating coupled evanescent wave biosensor;

Figure 2 is a plot of effective reflective index versus waveguide film thickness for the TE_0 mode for conventional and reverse symmetry waveguides;

Figure 3 is a plot of cover and substrate penetration depths in such systems;

Figure 4 is a plot of add layer sensitivities against waveguide film thickness in such systems;

Figure 5 is a plot of cover index sensitivities against waveguide film thickness for such systems;

Figure 6 shown in schematic exploded perspective view a preferred waveguide sensor unit of the invention;

Figure 7 is a schematic side view of a sensor of the invention incorporating a flow cell;

Figure 8 shows stages in a preferred manufacturing process for making waveguide sensor units of the invention;

Figure 9(a) and (b) are CCD photomicrographs under white light of two waveguide chips made by the method of Figure 8; and

Figure 10 shows similar views of the waveguide chips illuminated by a HeNe laser.

Figure 11 depicts sensitivity windows for the TE_2 and TM_2 modes in the free-standing waveguide implementation of reverse symmetry (n_F=1.56, n_S=1, n_C=1.333) and the dependence of the size of the sensitivity window on the mode number and polarization (inset).

Figure 12 shows theoretical calculations of the combined effects on the TE_0 mode of waveguide film thickness and waveguide refractive index with respect to (a) cover medium

penetration depth, (b) sensitivity to changes in the cover medium refractive index, and (c) the maximum detectable change in the cover medium refractive index. The film support is a mesoporous silica (n_S=1.15) and the cover medium is aqueous (n_C=1.333).

Figure 13(a) shows calculations of the cover medium penetration depths and refractive index sensitivity of a TiO_2-SiO_2 waveguide film (n_F=1.75) on glass (n_S=1.471) in an aqueous environment show zero sensitivity at the film thickness corresponding to the maximum penetration depth. (b) Using the same model system, the waveguide film cut-off thickness is predicted to decrease for small increments of the cover medium refractive index when the configuration has normal symmetry while the cut-off thickness increases monotonously with changes in the refractive index ones the configuration has attained reverse symmetry.

Figure 14 shows in graphical form design considerations for a specific application of monitoring cell attachment call for a maximum detectable cover medium refractive index change of at least 0.07. (a) The model system consists of a mesoporous silica supported polymer film for which the waveguide film thickness must be larger than 125 nm to attain this refractive index change window for the TE_0 mode. (b) The applicable range of film thicknesses yields probing depths up to 500 nm with high refractive index sensitivity using this configuration.

Figure 15 graphically illustrates that reverse symmetry free-standing waveguides benefit from the use of thicker waveguide films to improve their mechanical stability. Higher order modes can be used with micron thick waveguide films.

(a) The TE_2 mode of a free-standing polymer film (n_F=1.56) requires a film thickness of more than 1050 nm to ensure a maximum detectable cover medium refractive index change of at least 0.07. (b) The applicable range of film thicknesses provides probing depths up to 300 nm with a relatively high refractive index sensitivity.

Detailed description of the invention

Basic waveguide characteristics

As above, let us start with the essential part of the waveguide sensor: the waveguide module shown schematically in Fig. 1. In Figure 1, the numbered features are as follows:

100: Cover medium
101: Film
102: Substrate
103: Cover tail
104: Substrate tail
105: Light source
106: Grating coupler
107: Detector
108: Light mode
109: Angle of incidence

Following the electromagnetic theory developed for optical wave propagation in waveguide sensors (K. Tiefenthaler and W. Lukosz, Journal of the Optical Society of

America B, 6 (1989) 209-220), it may be found that to act as a waveguide, two conditions need to be fulfilled: (i) the refractive index of the film (101) has to be at least 1 % larger than the surrounding substrate and cover refractive indices, and (ii) the thickness of the film needs to be larger than a certain value called the cut-off thickness, d_{cutoff}, which may be found from the following expression (K. Tiefenthaler and W. Lukosz, Journal of the Optical Society of America B, 6 (1989) 209-220):

$$d_{cutoff} = \frac{1}{k\left(n_F^2 - n_{\max}^2\right)^{0.5}}\left(\arctan\left[\left(\frac{n_F}{n_{\min}}\right)^{2\rho}\left(\frac{n_{\max}^2 - n_{\min}^2}{n_F^2 - n_{\max}^2}\right)^{0.5}\right] + \pi m\right) \quad , \quad (1)$$

where k is the vacuum wavenumber of the light, n_F is the refractive index of the film, $n_{max} = \mathrm{Max}\{n_S, n_C\}$ is the largest of the refractive indices of the substrate, n_S, and the cover, n_C, respectively, $n_{min} = \mathrm{Min}\{n_S, n_C\}$ is the smallest of the refractive indices of the substrate and cover, respectively, ρ is the mode index which equals 1 for a transverse electric (TE) mode and 0 for a transverse magnetic (TM) mode, and m = 0, 1, 2, 3, ... is an integer representing the mode number.

If the two conditions (i) and (ii) are met, light propagation within the film is confined by total internal reflection at the substrate-film and cover-film interfaces. The confinement implies that the light, instead of being considered as rays bouncing back and forth between the two interfaces, may be viewed as one (or more) mode(s) of light, which all have directions of propagation parallel with the film.

Confinement does not mean, however, that there is no light present at all in the substrate and cover media. Any total internal reflection is accompanied by an exponentially decaying (evanescent) tail of light, which extends into the low-refractive-index medium, thus, in the present case into both the substrate and cover media. Therefore, the light modes propagating along the waveguiding film all have transversal amplitude profiles with light tails (103, 104) that extend (penetrate) exponentially into the substrate (102) and cover (100) media. The penetration depths of the two tails are denoted d_S and d_C for the substrate and cover tails, respectively.

Since the evanescent tails of the light modes propagate in the substrate and cover media but still along the film, the light modes experience or sense all three media at the same time. It means that the refractive index experienced by the travelling light modes is a weighed mixture of the three refractive indices, called the effective refractive index, N, which may be found from the following mode equation (K. Tiefenthaler and W. Lukosz, Journal of the Optical Society of America B, 6 (1989) 209-220):

$$d_F k\sqrt{n_F^2 - N^2} - m\pi = \arctan\left[\left(\frac{n_F}{n_S}\right)^2\left(\frac{N^2 - n_S^2}{n_F^2 - N^2}\right)^{0.5}\right] + \arctan\left[\left(\frac{n_F}{n_C}\right)^2\left(\frac{N^2 - n_C^2}{n_F^2 - N^2}\right)^{0.5}\right], \quad (2)$$

where d_F is the film thickness.

In the case of a four layer system where there is a very thin adlayer, e.g. of protein, between the film and the cover, N is derivable from the mode equation 2a below.

The guided waves or modes in a planar waveguide are TE_m (transverse electric or s polarized) and TM_m (transverse magnetic or p-polarized), where m = 0, 1, 2 ... is the mode number. Besides the mode number and polarization the modes can be characterized by their effective refractive index, denoted N. The effective refractive index can be calculated numerically from the mode equation, which can be written in the following form for a four-layer waveguide:

$$\pi m \cong k(n_F^2 - N^2)^{0.5}\left(d_F + d_A \frac{n_A^2 - n_C^2}{n_F^2 - n_C^2}\left[\frac{(N/n_C)^2 + (N/n_A)^2 - 1}{(N/n_C)^2 + (N/n_F)^2 - 1}\right]^{\rho}\right) - \arctan\left[\left(\frac{n_F}{n_S}\right)^2\left(\frac{N^2 - n_S^2}{n_F^2 - N^2}\right)^{0.5}\right] - \arctan\left[\left(\frac{n_F}{n_C}\right)^2\left(\frac{N^2 - n_C^2}{n_F^2 - N^2}\right)^{0.5}\right]. \quad (2a)$$

Here, $k = 2\pi/\lambda$, where λ is the vacuum wavelength of the guided light. The four layers of the waveguide are: the substrate (refractive index n_S), the waveguide film (refractive index n_F and thickness d_F), a thin adlayer on the waveguide film (refractive index n_A and thickness d_A) and the cover medium (refractive index n_C). ρ is a mode type number which equals 1 for TE and 0 for TM modes. Eq. (1) was derived under the assumption of a thin adlayer compared to the wavelength of the light ($d_A << \lambda$).

In the following, we choose, as a representative state-of-the-art conventional symmetry waveguide, a glass substrate (n = 1.471), a SiO_2-TiO_2 film (n = 1.75), and an aqueous cover (n = 1.333); as a representative for the reverse

symmetry waveguide of the invention we choose an air substrate (n = 1), a polymer film (n = 1.56), and an aqueous cover (n = 1.333). For these waveguides, the effective refractive index of the TE_0 mode exhibits a dependence on d_F as shown in Fig. 2. Here it is seen that when increasing d_F from the cut-off thickness (which is different for the two waveguides) to infinity, N goes from 1.471 (glass refractive index) to 1.75 (SiO_2-TiO_2 index) for the conventional waveguide, whereas N goes from 1.333 (water index) to 1.56 (polymer index) for the reverse symmetry waveguide. This shows that, for both waveguides, when d_F is increased well above the cut-off thickness, most of the light power propagates in the film layer, since $N \rightarrow n_F$. However, at the lower limit, when d_F approaches cut-off, the majority of the light power flows in the *substrate* for the conventional waveguide (because $N \rightarrow n_{glass}$), but for the reverse symmetry waveguide the light power is mainly propagating in the *cover* medium (because $N \rightarrow n_{water}$).

To explore this further, one may consult the equations for the penetration depths of the substrate and cover evanescent tails, which may be cast in the form (K. Tiefenthaler and W. Lukosz, Journal of the Optical Society of America B, 6 (1989) 209-220):

$$d_{s,c} = \frac{1-\rho}{k(N^2 - n_{s,c}^2)^{0.5}} + \frac{\rho\left[(N/n_F)^2 + (N/n_{s,c})^2 - 1\right]^{-1}}{k(N^2 - n_{s,c}^2)^{0.5}} \quad , \qquad (3)$$

Using again the TE_0 mode, $d_{s,c}$ show the dependencies on d_F depicted in Fig. 3. Here, it is clearly seen that when d_F approaches the cut-off thicknesses of the two waveguides, the

cover penetration depth of the reverse symmetry waveguide significantly exceeds the cover penetration depth of the conventional waveguide. Furthermore, simply by varying d_F, the thickness of the film, the probing depth in the cover of the reverse symmetry waveguide may be controlled with no upper limit. This is opposed to the conventional waveguide, in which the cover penetration depth has an upper limit, in Fig. 3 it may be found to be about 175 nm.

Principles of operation and applications

The main objective of optical waveguide biosensors is to transduce biological, biochemical, or chemical reactions in the cover medium into a measurable change in the optical properties of the guided light or to use the evanescent tail of the guided light in the cover material to induce observable changes there. A majority of the reactions considered take place at the film surface, which is usually chemically modified by the application of a biorecognition (affinity) layer. A variety of biorecognition layers are used in the art including antibodies, antigens, enzymes, receptors, proteins, lectins, organelles, and membrane bound chemoreceptors. Such types of biorecognition layers are capable of selectively binding their respective analytes to varying extents characterised by a binding constant if they are present in the cover medium, such as antigens, antibodies, hormones, neurotransmitters, opiates, amino acids, drugs, steroids, glucose, viruses, DNA/RNA fragments, and cells (O. Thordsen and R. Freitag in Biosensors in Analytical Biotechnology, edited by R. Freitag, 1996, R.G.

Landes Company and Academic Press, Inc, Chapter 3; N. Athanassopoulou and C. Maule, Physics World, 12 (1999) 19-20, S. -Y. Li et al. Biotechnological Progress, 10 (1994) 520-524).

Apart from the biorecognition layer sensors in which the recognition layer is rather thin and the bound analytes form a simple layer (adlayer) on top of the recognition layer, there are also sensors in the art that use a thicker biorecognition matrix (such as e.g. carboxymethyl dextran or geltec) with the actual biorecognition elements incorporated in the matrix. The analytes are then meant to penetrate the matrix and bind to the recognition elements (D. Yeung et al. Trends in Analytical Chemistry, 14 (1995) 49-56). The objective is here to increase the sensor response by adding detection events from the full penetration depth of the probing evanescent field.

The importance of the penetration depth of the cover evanescent field is evident, because to obtain a high sensitivity to adlayer growth, as much of the total light power has to propagate in the adlayer (K. Tiefenthaler and W. Lukosz, Journal of the Optical Society of America B, 6 (1989) 209-220). Therefore, when it comes to sensing small analyte elements, such as, for example, DNA fragments (typical size ~ 1 - 10 nm) or proteins (typical size ~ 3 - 50 nm), the conventional waveguide sensors with cover penetration depths on the order of, say, 100 nm exhibit high adlayer sensitivities. However, as the size of the analytes increases to the size of e.g. bacteria (~ 100 - 5000 nm) or cells (~ 1 - 10 μm), a similar cover penetration depth is needed to keep

a high sensitivity. In the art this is not possible with the known waveguide symmetries.

There are three main types of interaction between the guided light mode and the adlayer, used in transducing the adlayer formation into measurable optical parameters.

The first one is the adlayer's alteration of the effective refractive index of the guided light mode. Because the guided light mode has a transversal amplitude profile that covers all layers, i.e. substrate, film, adlayer, and cover, the effective refractive index of the mode is a weighed sum of the refractive indices of the individual layers, where the weighing depends on the mode's distribution of power among the four layers. Hence, as the refractive indices of the four layers are assumed to be known as well as the thickness of the film, it is possible from a measurement of the effective refractive index, N, to deduce the adlayer thickness.

There are two common ways of detecting N: by interferometry (US Pat. No. 4,950,074; US Pat. No. 5,465,151) or by in- and/or outcoupling from the waveguide (US Pat. No. 5,071,248; EP Pat. No. 0226604; WO Pat. No. 93/01487, WO Pat. No. 92/21976). In the first case, the waveguide is split into two arms, of which only one has a biorecognition layer on it. Hence, the light mode propagating in this arm experiences a shift in phase, due to the change in N, with respect to the other arm. This phase shift may be detected by joining the two arms again letting the modes interfere. N can then be deducted by measuring the light intensity of the interfering modes.

In- or outcoupling from the waveguide may be obtained using either gratings or a prism. In case of grating couplers, the following relation needs to be fulfilled to obtain efficient coupling into or out from the waveguide:

$$\sin(\theta) = N - \frac{\lambda}{\Lambda}, \qquad (4)$$

where θ is the angle of incidence of the external light beam, see Fig. 4 (212), or (in case of outcoupling) the exit angle from the waveguide, λ is the vacuum wavelength of the light used, and Λ is the grating period. Similarly, in case of prism coupling, the condition

$$\sin(\theta) = \frac{N}{n_p},$$

has to be fulfilled to obtain maximum coupling into or out from the waveguide where θ is the angle of incidence or angle of exit measured in the prism and n_p is the refractive index of the prism. The numbered features in Figure 4 are as follows:

204: Light source

205: Substrate

206: Substrate tail

207: Grating coupler

208: Air groove

209: Detector

210: Aqueous cover (flow cell)

211: Cover tail

212: Angle of incidence

Hence, by measuring the intensity of the in- or outcoupled light by a detector, see, for example, Fig. 4, and by using Eqs. 4 and 5 one can determine *N* from the angle at which maximum in- or outcoupling is obtained.

Returning to the other two main types of interaction between the guided light mode and the adlayer, a second is the adlayer's total or spectral absorption of the guided light mode (B. Zimmermann et al. Sensors and Actuators B, 41 (1997) 45-54; US Pat. No. 5,082,629). The cover tail's propagation in the adlayer may lead to absorption of the guided light mode. Moreover, the absorption may be wavelength dependent. This means that by coupling a broad, homogeneous spectrum of light into the waveguide and then after the interaction with the adlayer measuring the wavelength spectrum of the light, it may be possible from this spectrum to identify and/or quantify certain substances in the adlayer, namely the ones that absorb light in the wavelength range missing in the analysed spectrum.

Finally, the last typical type of interaction is fluorescence spectroscopy (Zhou et al., Biosensors and Bioelectronics, 6 (1991) 595-607; WO Pat. No. 90/06503, US Pat. No. 5,959,292), in which the evanescent cover light tail photoexcites the immobilised molecules at the film surface. The fluorescence from these molecules may couple back into the waveguide after which it can be measured by a detector, for example at the end facet of the waveguide. By analysing the fluorescence spectrum it may be possible to identify and/or quantify the substances in the adlayer, namely the ones that fluoresce light in the wavelength range appearing in the analysed spectrum.

The three interaction methods all make it possible to perform qualitative, quantitative, and even kinetic measurements and monitoring of the adhesion of analytes.

Sensitivities

For the detection of thin adlayers, the conventional waveguide is known to have a very high sensitivity. How is this for the reverse symmetry waveguide? To analyze this we use the expression for the adlayer sensitivity for an infinitely thin addlayer (K. Tiefenthaler and W. Lukosz, Journal of the Optical Society of America B, 6 (1989) 209-220):

$$\frac{\partial N}{\partial d_A} = \frac{n_F^2 - N^2}{N d_{eff}} \frac{n_A^2 - n_C^2}{n_F^2 - n_C^2} \left[\frac{(N/n_C)^2 + (N/n_A^2) - 1}{(N/n_C)^2 + (N/n_F^2) - 1} \right]^p , \qquad (6)$$

where n_A is the refractive index of the addlayer and $d_{eff} = d_S + d_F + d_C$ is the effective waveguide thickness. The sensitivity $\partial N/\partial d_A$ is defined by the relative change in effective refractive index N per initial increase in addlayer thickness, d_A. In Fig. 5 the adlayer sensitivity is plotted versus film thickness for the two model conventional and reverse symmetry waveguides, again for the TE_0 mode. It is seen that the adlayer sensitivity for the reverse symmetry waveguide actually has a higher peak value ($4.6 \cdot 10^{-4}$ nm^{-1}) than that for the conventional one ($3.7 \cdot 10^{-4}$ nm^{-1}) . Also, it is seen that the peak value is obtained for a thicker film (250 nm) for the reverse symmetry waveguide than for the conventional one (180 nm), which may be an advantage in terms

of manufacturing. Finally, it seems obvious, even though we have no theoretical evidence, that as the adlayer builds up, the adlayer sensitivity for the conventional waveguide must drop off quicker than for the reverse symmetry waveguide. This simply because in the conventional waveguide, a thin adlayer of, say, 100 - 200 nm is enough to accommodate all of the cover tail. In the reverse symmetry case, where the cover tail may be up to several microns, this total adlayer accommodation of the cover tail must occur for much thicker addlayers. In conclusion, the dynamic range of the reverse symmetry waveguide is expected to be considerably larger than for the conventional waveguide.

Apart from the adlayer sensitivity, there is the cover refractive index sensitivity, which represents the second important feature of waveguide sensors. This sensitivity is given by (K. Tiefenthaler and W. Lukosz, Journal of the Optical Society of America B, 6 (1989) 209-220):

$$\frac{\partial N}{\partial n_C} = \frac{n_C}{N}\left[\frac{n_F^2 - N^2}{n_F^2 - n_C^2}\right]\frac{d_C}{d_{eff}}\left[2\frac{N^2}{n_C^2} - 1\right]^{\rho}, \qquad (7)$$

and represents the change in effective refractive index per change in cover index (in the absence of an adlayer). These sensitivities are shown for the conventional and reverse symmetry waveguides in Fig. 6. As is seen, the cover refractive index sensitivity for the reverse symmetry waveguide is generally much higher (up to a factor of 5) than that of the conventional waveguide. This is simply due to the fact, that in the reverse symmetry waveguide, a much

larger fraction of the guided light mode power flows in the cover.

When the waveguide is used as an evanescent wave sensor the monitored quantity is N and its change (ΔN) is the sensor response to the change of any parameter of the waveguide environment. If the change of a parameter is small, the resulting change in the effective refractive index can be described to first order by:

$$\Delta N = \sum_i (\partial N / \partial x_i) \Delta x_i, \qquad (8)$$

where $x_i = \{n_S, n_F, d_F, n_C, n_A, d_A\}$

The minimum detectable ΔN is given by the measurement set-up. If light is coupled into the waveguide by a surface relief grating, N can be calculated from the incoupling angle. The precision of the incoupling angle measurement consequently determines the minimum detectable ΔN. The partial differentials in Eq. (8) are given by the waveguide structure and should be maximized through the waveguide design to be able to detect small changes in x_i with a given set-up. Therefore, these quantities are termed the sensor sensitivities for x_i, for which we use the notation $S\{x_i\} \equiv \partial N / \partial x_i$.

Most common waveguide sensor applications monitor changes in n_C or in d_A, in the former case using the waveguide as a differential refractometer for liquid refractive index sensing and in the latter case as a

biosensor to follow, for example, protein adsorption. Tiefenthaler and Lukosz derived the following expressions for the sensitivities $S\{n_C\}$ and $S\{d_A\}$:

$$S\{n_C\} = \frac{n_C}{N}\left[\frac{n_F^2 - N^2}{n_F^2 - n_C^2}\right]\frac{\Delta z_{F,C}}{d_{eff}}\left[2\frac{N^2}{n_C^2} - 1\right]^{\rho}, \qquad (9)$$

$$S\{d_A\} = \frac{n_F^2 - N^2}{N d_{eff}}\frac{n_A^2 - n_C^2}{n_F^2 - n_C^2}\left[\frac{(N/n_C)^2 + (N/n_A^2) - 1}{(N/n_C)^2 + (N/n_F^2) - 1}\right]^{\rho}, \qquad (10)$$

where d_{eff} is the effective waveguide thickness given by:

$$d_{eff} = d_F + \sum_{J=S,C} \Delta z_{F,J}, \qquad (11)$$

where

$$\Delta z_{F,J} = \frac{1-\rho}{k(N^2 - n_J^2)^{0.5}} + \frac{\rho\left[(N/n_F)^2 + (N/n_J^2) - 1\right]^{-1}}{k(N^2 - n_J^2)^{0.5}}, \qquad (12)$$

is the penetration depth of the waveguide mode with high intensity into the substrate (J=S) or cover medium (J=C). Equation (10) was derived in the limit $d_A \rightarrow 0$, i.e. for thin adlayers and the same result was derived from perturbation theory. The authors of this work concluded that a large part of the guided wave power should propagate in the adlayer / cover medium to reach high sensitivity to analytes. Although

this rule gives a picture of proportionality between the power and the sensitivities, we note here that the proportionality factor between $S\{n_c\}$ and the fraction of power propagating in the cover medium could be larger than 1 in special cases for the TM modes leading to $S\{n_c\}$ being larger than 1.

A given mode type propagates only as a guided wave if the thickness of the waveguide film is larger than a well-defined value, called the cutoff thickness d_c (Eq 1). It is known that when the film thickness approaches the cutoff thickness ($d_F \rightarrow d_c$), the effective refractive index, N, of the mode under study approaches n_{max}. Furthermore, Eq. (12) implies that the penetration depth goes to infinity at the cutoff point on the side of the film that has the bigger refractive index, while the penetration depth will be finite on the other side. The effective waveguide thickness will also be infinite in this case, *cf.* Eq (11). In a normal symmetry waveguide biosensor, n_{max} is by definition always equal to n_s.

We now summarise the most important theoretical differences between normal and reverse symmetry waveguides and discuss important practical issues to consider in actual sensor implementations.

If the cover refractive index increases due to adsorption of, for example, cells, the cut-off thickness will increase too, according to Eq. 1. This implies that the curves of Fig. 5 will be shifted to the right, i.e. larger film thickness. Consequently, $S\{n_c\}$ will be larger for every mode for a given film thickness. The cut-off thickness of the probing mode may eventually be larger than the film

thickness leading to disappearance of the mode in the waveguide. In most applications, we would like to maintain high sensitivity at all analyte concentrations. We define a sensitivity window, w, of waveguide film thicknesses where $S\{n_c\}$ is in the range between 0.2 and 1. The size of this window is important for actual sensor applications, as it has a close relationship with the fabrication accuracy of the film thickness required to reach high sensitivity. Fig. 11 shows the wide $S\{n_c\}$ range of the second order modes in the free-standing waveguide implementation, as an example. The inset shows the size of the sensitivity window depending on the polarization and mode number. Using the defined sensitivity window one can estimate the maximum cover refractive index change (Δn_c^{high}) that can be monitored by a sensor with sensitivities between 0.2 and 1:

$$w = d_c(n_c + \Delta n_c^{high}) - d_c(n_c) \quad (13)$$

Δn_c^{high} is around 0.05 for the TM_2 mode of a free-standing polymer film and around 0.11 for the TM_0 mode of a mesoporous silica supported polymer film. This range decreases with increasing mode number implying that a larger n_c range can be probed with high sensitivity using the lower order modes. This property of reverse symmetry waveguides should be considered in sensor applications. The possibility to exceed the cut-off thickness locally by attachment of, for example, cells in a controlled way may have interesting analytical

applications. The exact behavior of such a system will need further theoretical and experimental work to be explored.

The combined effects of thickness and refractive index of the waveguide film are demonstrated in figure 12a,b and c using the TE_0 mode of a mesoporous silica (n_s=1.15) supported film in an aqueous environment (n_c=1.333) as an example. The penetration depth of the mode into the cover medium, its sensitivity to refractive index changes and the maximum detectable cover medium refractive index range (Δn_c^{max}) have been calculated for a range of different film refractive indices from 1.4 to 1.8. The calculated curves show that that the sensitivity $S\{n_c\}$ increases with increasing probing depth for a reverse symmetry waveguide. The probing depths have strong singularities at the cut-off film thickness. For infinitely thick waveguide films, the probing depths become constant and this constant is larger for smaller film refractive indices (this is also clear from Eq. 12). The singularity at the cut-off thickness is sharper for larger film-cover medium refractive index contrasts. From a manufacturing point of view, a high refractive index contrast will be a disadvantage if the aim is to make a waveguide with high penetration depth and high analyte sensitivity since the film thickness should be smaller and must be produced with higher accuracy. This would suggest that small refractive index contrast should be favored in general. The singularity at the cut-off thickness has a correspondingly strong effect on the maximum detectable refractive index range as shown in figure 12c. A waveguide film thickness close to the cut-off thickness results in a small detectable n_c range, approaching zero at the cut-off point. At infinite film thickness, the

maximum detectable range is equal to the difference between the film and cover medium refractive indices, implying that a smaller refractive index contrast results in a smaller detectable cover medium refractive index range. The selected film thickness and refractive index is consequently a compromise between large Δn_C^{max} and high sensitivity / probing depth, and should be optimized for each application.

The observation that $S\{n_C\}$ increases monotonously with increasing probing depth for all film thicknesses is only valid for reverse symmetry waveguides. Figure 13a presents calculated cover medium penetration depths and sensitivities to the cover medium index change for the TM_0 mode of the normal symmetry TiO_2-SiO_2 waveguide film (n_F=1.75) on glass (n_S=1.471) sensor. The probing depth is seen to have a theoretical maximum of approximately 180 nm. However, the sensitivity to changes in the cover medium refractive index (analyte) is zero for this film thickness due to the strongly increasing penetration depth into the film substrate at the cut-off film thickness. This implies that actual waveguide sensors normally will be designed to optimize sensitivity (in this example at a waveguide film thickness of 200 nm) rather than maximize probing depth.

The addition of analytes to an aqueous cover medium phase will lead to an increase in the effective cover medium refractive index. We have calculated the effect of such an increase on the cut-off waveguide film thickness for a TiO_2-SiO_2 waveguide film (n_F=1.75) on glass (n_S=1.471) (see Fig. 13b). For smaller increments of the cover medium refractive index, the waveguide has normal symmetry yielding reduced cut-off thicknesses. This thickness reaches zero for a

symmetrical waveguide configuration (n_c=n_s). The monotonous reduction in cut-off thickness implies that the probing mode will never disappear in a normal symmetry waveguide. Beyond the symmetrical configuration, the waveguide has reverse symmetry giving a monotonously increasing cut-off thickness with increasing n_c. In this region, the cut-off thickness may become larger than the actual film thickness thereby leading to disappearance of the probing mode.

The increased sensitivity to analytes is not the only important perspective of these structures, in our opinion. The reverse symmetry configuration should overcome problems of evanescent wave sensing of living cells and bacteria. The previously mentioned TiO_2-SiO_2 waveguides have been used for monitoring of living cell attachment and spreading. The penetration depths of such normal symmetry sensors into the cover medium are 100-200 nm (180 nm for the TM_0 mode) as discussed above and can merely detect the bottom part of higher cells (diameter ~ 10 µm) or bacteria (diameter ~ 1 µm). The measured quantity is mainly related to the contact area between the organism and the surface, but not to the morphology or refractive index of the whole organism. Moreover, even if a higher cell is completely attached to the surface only its sparse points of attachments can be found within 100-200 nm from the surface, thus giving a very small measurable refractive index change. Reverse symmetry waveguides overcome this limitation. The ability to increase the probing depth beyond 200-300 nm, while retaining high sensitivity, will be a major advantage for detection of such micron scale tall objects.

For an actual sensor application using reverse symmetry waveguides, it is required to know the maximum change in cover medium refractive index, Δn_c^{max}, that must be detectable. This number will strongly influence the attainable sensitivity and depth at the starting point of the sensing process. As an example, the interior of a cell attaching to the sensor surface will have an effective refractive index of less than 1.40, even with a large margin. This implies that the Δn_c^{max} should be at least $1.40-1.333 \approx 0.07$ if one wishes to follow the whole attachment process. Taking $\Delta n_c^{max} > 0.07$, Fig. 14a shows that the film thickness should be bigger than 125nm for the TE_0 mode of a mesoporous silica ($n_s=1.15$) supported polymer film ($n_F=1.56$). This film range has a maximal probing depth of 500 nm and $S\{n_c\}=0.6$ (Fig. 14b). If the film thickness is chosen somewhat thicker, say 240 nm, to avoid the strongly diverging region close to the cut-off thickness, actually, we can follow the whole cell attachment process with $S\{n_c\}$ between 0.2 and 0.6 and probing depth between 200 and 500 nm. This is much better than the values of the TiO_2-SiO_2 waveguides typically used nowadays.

The maximum $S\{n_c\}$ decreases with increasing mode number for normal symmetry waveguides, so it is preferable to use the zero order mode to monitor surface processes. This is not true for the reverse symmetry design. The maximum $S\{n_c\}$ is always 1. The window, w, of film thicknesses giving high sensitivities narrow for higher order modes (*cf.* Fig. 11), leading for sharper $S\{n_c\}$ curves. This places stronger demands on the fabrication precision of the film, but in terms of manufacturing it is easier to make thicker films. This is particularly true for free-standing waveguide films

where a thick film provides better mechanical stability. Taking the TE_2 mode of a free-standing polymer waveguide film (n_F=1.56) as an example, Fig 14 shows the calculated Δn_C^{max}, cover medium probing depth and $S\{n_C\}$ dependencies on the film thickness. If this film is used to follow attachment of higher cells, the film thickness should be at least 1060 nm based on a maximum detectable refractive index change of 0.07. For this system, the starting $S\{n_C\}$ is 0.15 and the starting probing depth is around 300 nm. These values are highly competitive with the classical TiO_2-SiO_2 sensor (*cf.* Fig. 12a).

Fabrication

The essential part of the invented sensor principle is the reverse symmetry of the optical waveguide. One suggestion to this design is shown in Figs. 4, 7 and 8. In Fig. 7, the substrate (205) consists of a block of UV-cured polymer, in which an air groove (208) of typically 0.5 - 6 mm's length, 10 - 200 µm's width, and 1 - 100 µm's depth is made. On top of that is glued or adhered a waveguiding film (202), made from the same type of UV cured polymer, and with a thickness of typically 100 - 1000 nm depending on the desired cover penetration depth. Prior to attachment, the bottom surface of the film is profiled with a surface relief grating (207) with a periodicity of typically 0.3-1 µm and a depth of typically 10 - 100 nm. The resulting waveguide chip is implemented in a traditional optical waveguide sensor system, of which the grating coupling system is shown as an example in Fig. 4. As is seen, the optical waveguide

operates in a reverse symmetry with an aqueous cover medium with refractive index 1.333, a film with a refractive index of a polymer (typically ~1.4 - 1.6), and a substrate consisting of air with a refractive index of 1.

Concerning fabrication of the waveguide chip, the procedure outlined in Fig. 8 has been tested. The fabrication consists of three separate steps: (i) fabrication of film with surface relief grating, (ii) fabrication of substrate with air groove, and (iii) assembling of the two parts.

In the film preparation (i), a master of the coupling grating was first manufactured in photoresist-on-glass. Here, a 2 μm thick photoresist film was exposed by the interference pattern formed by crossing two plane monochromatic laser beams originating from a HeCd laser. After development, this resulted in the formation of a sinusoidal surface relief pattern in the photoresist, in the present case it had a period of 500 nm and a depth of 100 nm. Polydimethylsiloxane (PDMS), Sylgard 184, Dow Corning was then poured on top of the photoresist grating and heat cured for 27 hours at 150°C. After separating the cured PDMS from the glass master, a negative replica of the original photoresist grating was formed in the PDMS. A plate of poly-vinyl-pyrrolidone PVP was now spincoated with a 4 μm thick layer of UV curable polymer, here a NOA 71, Norland Optical Adhesives, also referred to as UVCP, which is a mercaptoester based polymer. By positioning the PDMS master onto the UVCP film and afterwards partially curing (semi-cure) the UVCP by 10 min illumination from a UV lamp, it was possible to peel off the PDMS master and still obtain a stable replica of the

sinusoidal PDMS surface relief grating in the semi-cured UVCP film.

We measured the thickness of the cured polymer by profilometry. Polymer films cured without the elastomer mold were similarly characterized to determine the mechanical effect of the mold. These experiments showed some important characteristics of this fabrication method. (1) The elastomer mold does not only copy its surface relief onto the polymer film, it also decreases the film thickness. This effect mainly originates from the weight of the mold and increases with thicker molds. (2) The viscosity of the UV resin imposes a limit on the minimum film thickness. For NOA 72 (viscosity 155 cps) this minimum thickness is about 3 µm without the elastomer mold and about 1.6 µm with the elastomer mold. We overcame this limitation by diluting the UV resin with THF (purum, Sigma). Spin casting a solution of 1 mg/ml NOA 72 in THF resulted in cured film thicknesses of around 1 µm and 0.3 µm without and with the elastomer mold, respectively. The thickness range available through these techniques allow the fabrication of waveguides with mono- or multi-mode operation.

In the substrate fabrication (ii), a master of the air-groove was first manufactured in photoresist-on-glass. A glass plate was spincoated with an 8 µm thick film of negative photoresist (microresist SU8). After hard-baking, the resist was illuminated by UV-light through a metal mask with an opening of the same size as the desired grove, in this case 200 µm x 2 mm. After developing, the exposed photoresist was removed resulting in an air-grove of the desired dimension. After this, PDMS was poured on top of the

glass plate and cured for 27 hours at 150°C. Then, it was possible to separate the cured PDMS from the glass/ photoresist plate, resulting in a negative replica now being formed in the PDMS. Some UVCP was now poured on top of the PDMS master followed by UV exposure from a UV lamp, which semi-cured the UVCP. After separation of the UVCP from the PDMS master, a replica of the original photoresist air-groove was formed in the UVCP.

In the assembling step (iii) the semi-cured polymer film with the PVP substrate was put upside-down on top of the air-grooved substrate from step (i). This sandwich was then illuminated by the UV lamp again, to fully complete the curing of the UV curable film. Finally, the PVP substrate was dissolved in water, leaving the UV cured film with the surface relief grating as a closed sealing of the air-grove in the substrate.

This method may readily be adapted to produce arrays of waveguide film areas over respective air gaps.

Several examples of free-standing waveguides have been fabricated. In Fig. 9 two waveguide chips with arrays of free-standing waveguides are shown. To verify that the fabricated waveguides were really free-standing, we did two experiments. First, we simply illuminated the free-standing waveguides with white light. As a result, we observed light diffraction only at the positions of the air groves, see Figs. 9a and b. It means that the waveguide incorporating the grating is really free-standing; otherwise there would be no diffraction observed. Secondly, we tested the coupling properties by illuminating the waveguides with a HeNe laser beam. In this case we observed successful incoupling as well

as waveguiding all the way to the edge of the chip, see Fig. 10.

Alternative substrates

As alternatives to the air-grooved substrate described above, we also wish to mention the possibility of using a substrate that contains small cavities of air, like micropores or small air-filled nanostructures at the surface. Such nanostructures include grooves oriented in the direction of mode propagation with a spacing and periodicity much less than the wavelength of the light. The effective refractive index of the substrate for the TE and TM modes will be 1.19 and 1.31, respectively, for a nanostructured polymer support with refractive index 1.56 and grooves with equal widths of openings and substrate material.

In this case, if the dimensions of the microporosity or the nanostructures are well below the wavelength of light used, the guided light mode will simply "see" the substrate medium as an average between the substrate material and the air resulting in an apparent refractive index which is somewhere between that of the substrate and air. As a result, it may be possible, if the air to substrate volume ratio is sufficiently low, to obtain apparent substrate refractive indices less than that of water, i.e. < 1.333, and thereby obtain a reverse symmetry waveguide.

Thus, in summary, the invention has provided in its preferred aspects a reverse symmetry waveguide as a sensor module for optical biosensing. In the suggested reverse symmetry waveguide, the refractive index of the waveguiding

film is larger than the refractive indices of the substrate and cover media, but, in addition, the refractive index of the substrate is less than the refractive index of the cover medium, which for biosensor applications is mostly aqueous. The low substrate refractive index implies that the sensing evanescent tail of the guided light mode that penetrates into the cover can be infinite in extent resulting in a considerable improvement of in-depth sensitivity.

Claims

1. An optical waveguide sensor comprising a substrate material having a refractive index n_s , an optical waveguide film on the substrate material having a refractive index n_F , and a cover material over the waveguide having a refractive index n_c , a light source optically coupled to said waveguide, and a detector for detecting evanescent wave interaction between said light and said cover material, wherein $n_F > n_s$ and $n_F > n_c$ and $n_c > n_s$, and $n_c < 1.45$.

2. A sensor as claimed in claim 1, wherein $n_s < 1.3$.

3. A sensor as claimed in claim 1 or claim 2, wherein the cover material is an aqueous medium.

4. A sensor as claimed in any preceding claim, wherein the substrate material is a gas or a gas containing material.

5. A sensor as claimed in claim 4, wherein the substrate material is air or an air containing material.

6. A sensor as claimed in claim 4, wherein the substrate is air and is contained in an air space defined by an air groove in a solid material which is in physical contact with the waveguiding film and which has a depth larger than the air-substrate penetration depth of the light.

7. A sensor as claimed in claim 4, wherein the substrate material incorporates microporous or mesoporoous structures with refractive index variations on length scales smaller than the wavelength of light used for analysis.

8. A sensor as claimed in claim 4, wherein the substrate surface incorporates nano-structures with refractive index variations on length scales smaller than the wavelength of light used for analysis.

9. A sensor as claimed in any preceding claim, including a housing containing said cover material in contact with said waveguide, said housing having an inlet for the introduction of a sample for sensing.

10. A sensor as claimed in claim 9, wherein said housing forms a flow cell through which a said sample constituting said cover material can be flowed in use.

11. A sensor as claimed in any preceding claim, wherein the waveguiding film is constituted by a polymer film.

12. A sensor as claimed in claim 11, wherein said polymer film is light-cured.

13. A sensor as claimed in Claim 12, wherein said polymer film is combined with a possibly structured substrate made from the same polymer material.

14. A sensor as claimed in any preceding claim, wherein light from the light source is coupled into and/or out from the waveguide via coupling gratings incorporated in the waveguide.

15. A sensor as claimed in any preceding claim, wherein light from the light source is coupled into and/or out from the waveguide through an optical prism.

16. A sensor as claimed in any preceding claim, wherein light from the light source is coupled into and/or out from the waveguide through end facets of the waveguide.

17. A sensor as claimed in any preceding claim, wherein light is guided to and/or from the coupling elements through an optical fibre.

18. A sensor as claimed in any preceding claim, wherein the light from the light source which is incident on the waveguide film is a collimated light beam or a focused light beam.

19. A sensor as claimed in any preceding claim, wherein the light source is a laser or a monochromatic light source or a non-monochromatic light source.

20. A sensor as claimed in claim 18, wherein said light source is non-monochromatic.

21. An array of sensors claimed in any preceding claim, wherein at least one of the sensors in the array is for use as reference sensor.

22. An array of sensors claimed in claim 21, wherein different sensors have been chemically designed to react with different substances.

23. A method for sensing evanescent wave interaction between light and a sample material, comprising introducing said sample material as or into said cover material in a sensor as claimed in any preceding claim, and detecting said interaction using said detector of the sensor.

24. A method as claimed in claim 23, wherein said sample produces an alteration in said cover material at least 200 nm away from said waveguide, which alteration in said cover material is detected as a change in said evanescent wave interaction between said light and said cover material.

25. A method as claimed in claim 23 or claim 24, wherein said sample includes micro-organisms (prokaryotes) or biological cells (eukariotes) whose interaction with each other or with the waveguide surface changes the optical properties of said evanescent wave and the optical properties of the waveguided light.

26. A method of fabricating an optical waveguide sensor unit, comprising:

a) forming an optical coupling grating master by forming a layer of photoresist polymer on a surface, exposing said photoresist polymer to interfering monochromatic light beams such that interference fringes formed by said light beams expose the photoresist such that upon development the photoresist forms an optical grating pattern, developing said photoresist to form said optical grating pattern as said optical grating master,

b) casting a negative polymer impression of said master by applying a settable polymer thereto, setting said polymer and removing said polymer from said master,

c) contacting said negative polymer impression of the optical grating pattern into a light-curable polymer film supported by a temporary support substrate and partially curing the light-curable polymer followed by removal of said negative imprint of the optical grating leaving a positive replica of said optical grating pattern in the partially cured polymer film,

d) forming a master of a shallow groove by forming a layer of photoresist polymer on a surface, exposing said photoresist polymer to light such that said light exposes the photoresist in a desired groove pattern such that upon development the photoresist forms walls bordering a groove of which said surface forms a base, developing said photoresist to form said groove pattern as said groove master,

e) casting a negative impression of said groove master by applying a settable polymer thereto, setting said polymer and removing said polymer from said groove master,

f) casting a light-curable polymer onto said negative impression of the groove master and partially curing the same followed by removal of said partially cured polymer bearing a groove which is a positive replica of said groove master,

g) uniting said positive replica of the groove master and said positive replica of the optical grating pattern such that together they form a conduit having said film incorporating said optical grating pattern spanning said groove and completing the cure of said partially cured polymer, and

h) removing said temporary support substrate from the polymer film incorporating said optical grating pattern.

27. A method as claimed in claim 25, wherein each negative impression is formed in an elastomeric material.

28. A method as claimed in claim 25 or claim 26, wherein said temporary support substrate is formed of a soluble polymer and is removed by being dissolved in an appropriate solvent.

29. A method as claimed in any one of claims 26 to 28, wherein the masters of said optical grating pattern and said groove are used repeatedly in steps (b) and (e) of said method.

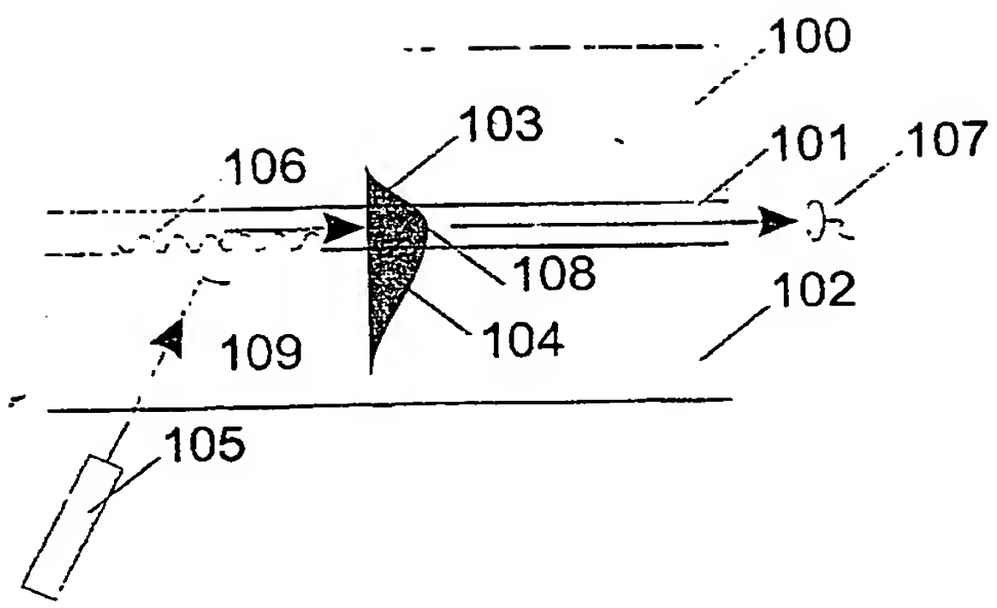

Figure 1

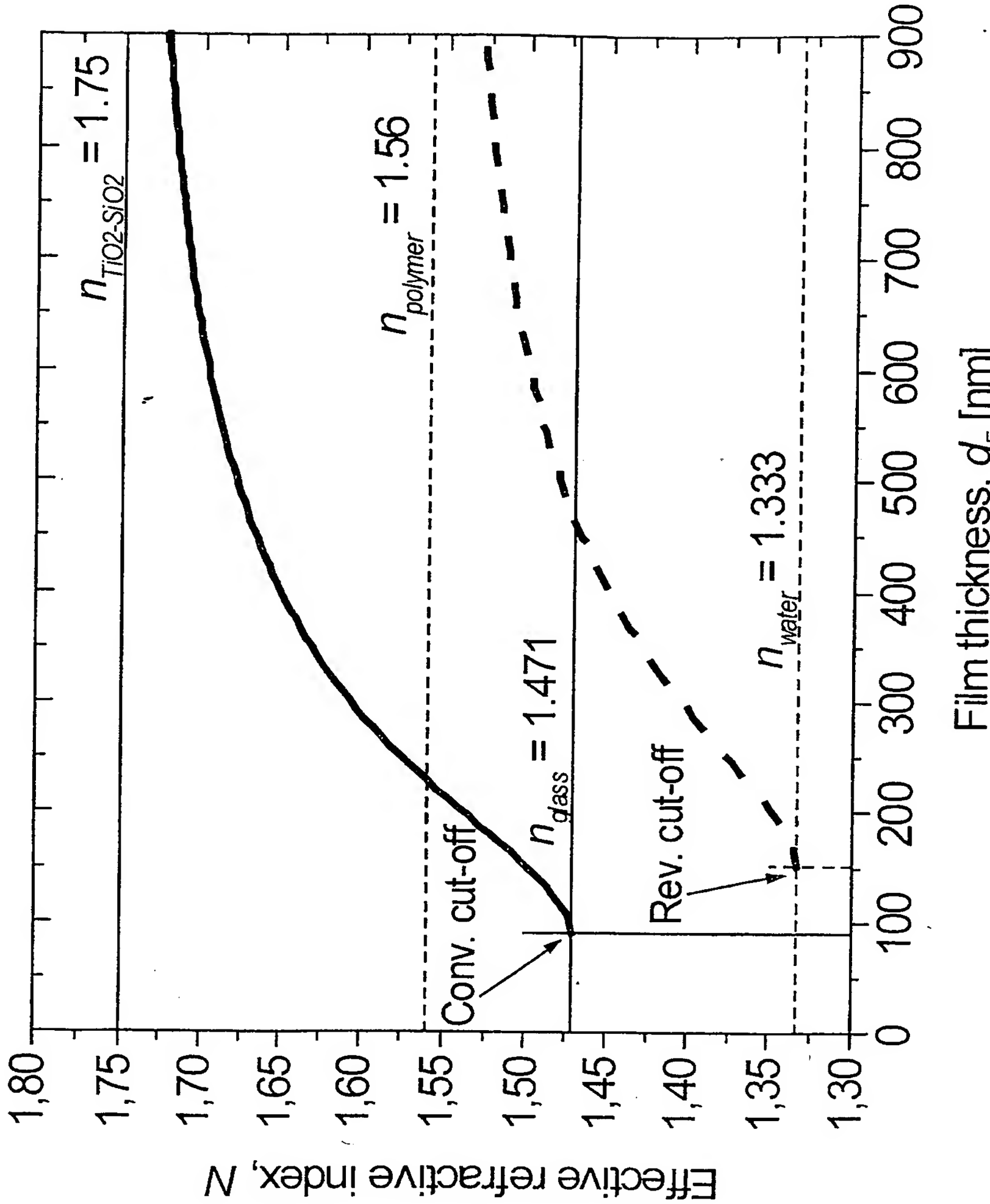
Effective refractive index, N
1,80
1,75
1,70
1,65
1,60
1,55
1,50
1,45
1,40
1,35
1,30
Film thickness, d_F [nm]
0
100
200
300
400
500
600
700
800
900
$n_{TiO2\text{-}SiO2}$ = 1.75
$n_{polymer}$ = 1.56
n_{glass} = 1.471
n_{water} = 1.333
Conv. cut-off
Rev. cut-off

Fig. 2

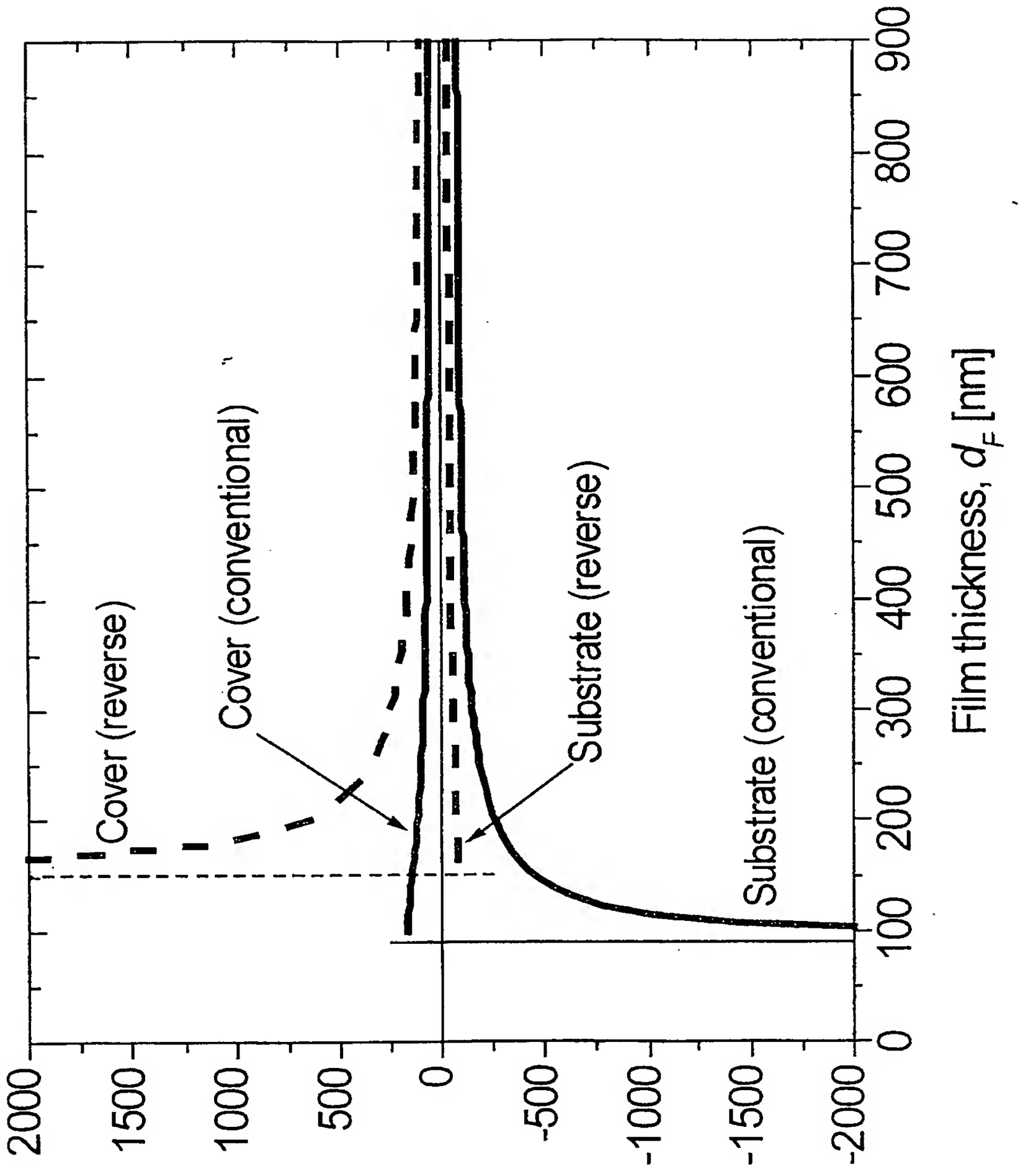
Cover (reverse)
Cover (conventional)
Substrate (reverse)
Substrate (conventional)
2000
1500
1000
500
0
-500
-1000
-1500
-2000
Penetration depths, $d_{S,C}$ [nm]
0
100
200
300
400
500
600
700
800
900
Film thickness, d_F [nm]

Fig. 3

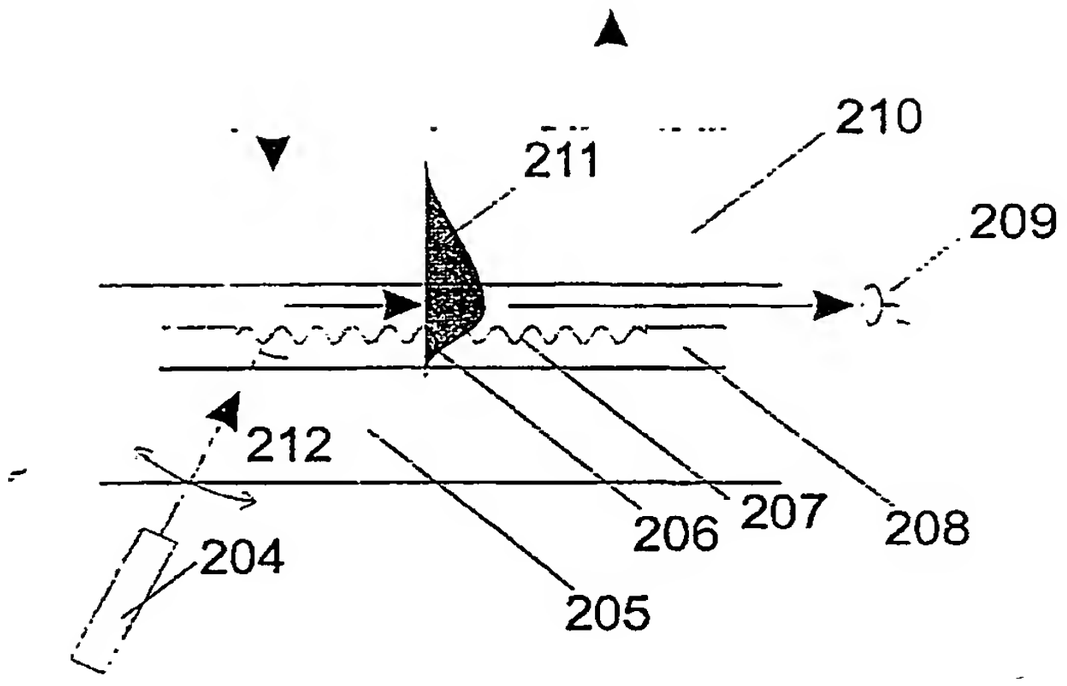

Figure 4

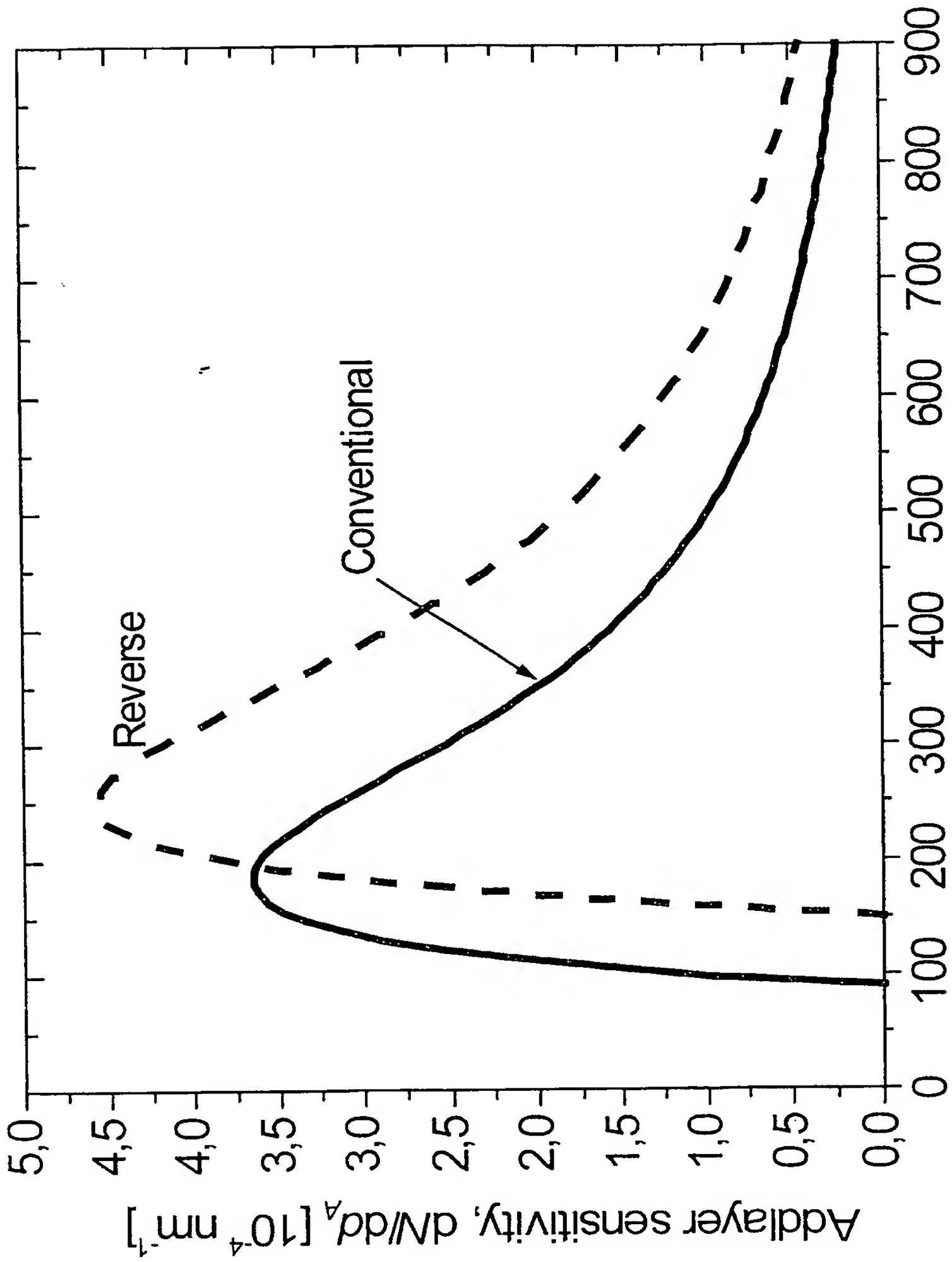
Addlayer sensitivity, dN/dd_A [10^{-4} nm^{-1}]
5,0
4,5
4,0
3,5
3,0
2,5
2,0
1,5
1,0
0,5
0,0
Film thickness, d_F [nm]
0
100
200
300
400
500
600
700
800
900
Conventional
Reverse

Fig. 5

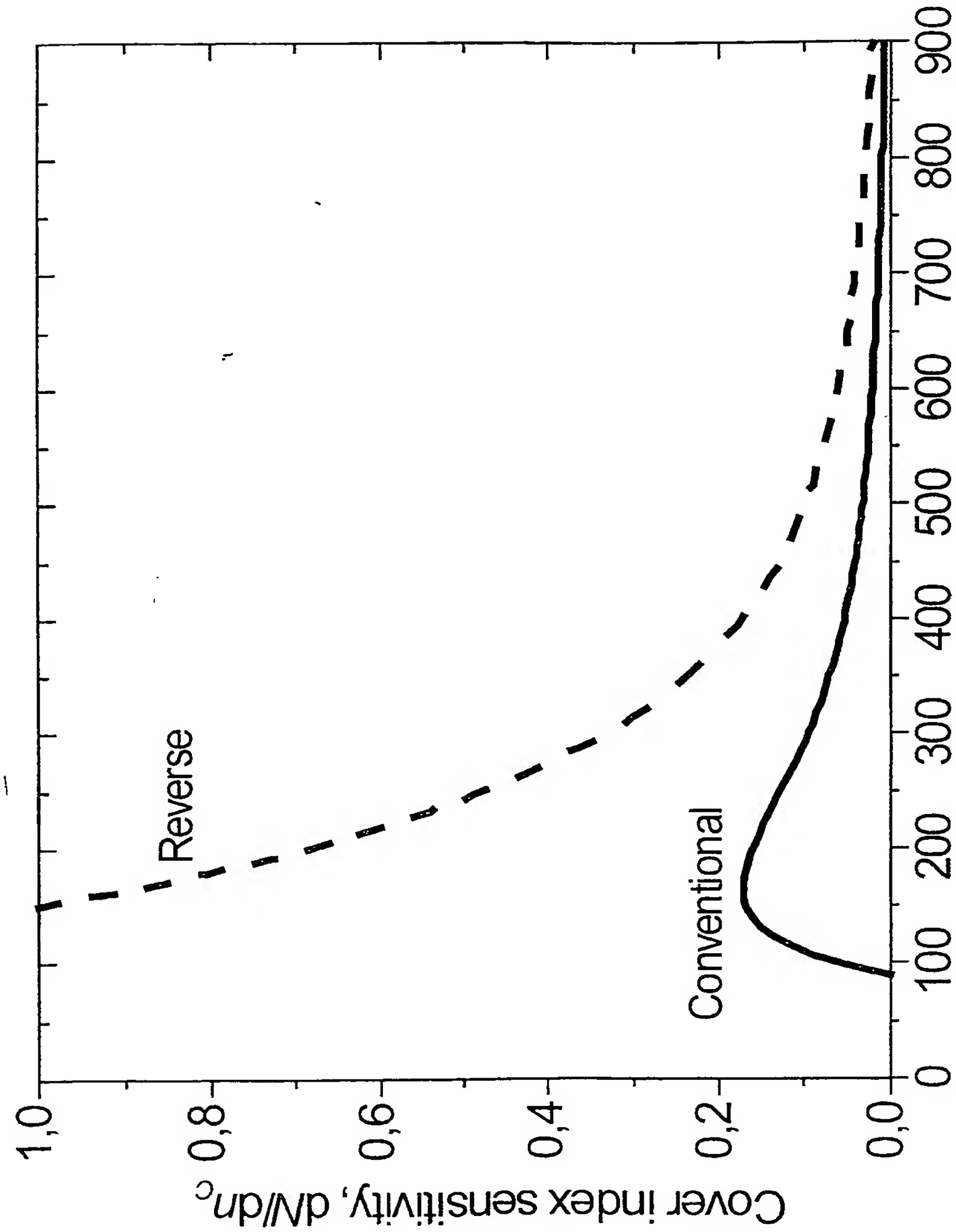
Film thickness, d_F [nm]
0
100
200
300
400
500
600
700
800
900
Cover index sensitivity, dN/dn_C
0,0
0,2
0,4
0,6
0,8
1,0
Conventional
Reverse

Fig. 6

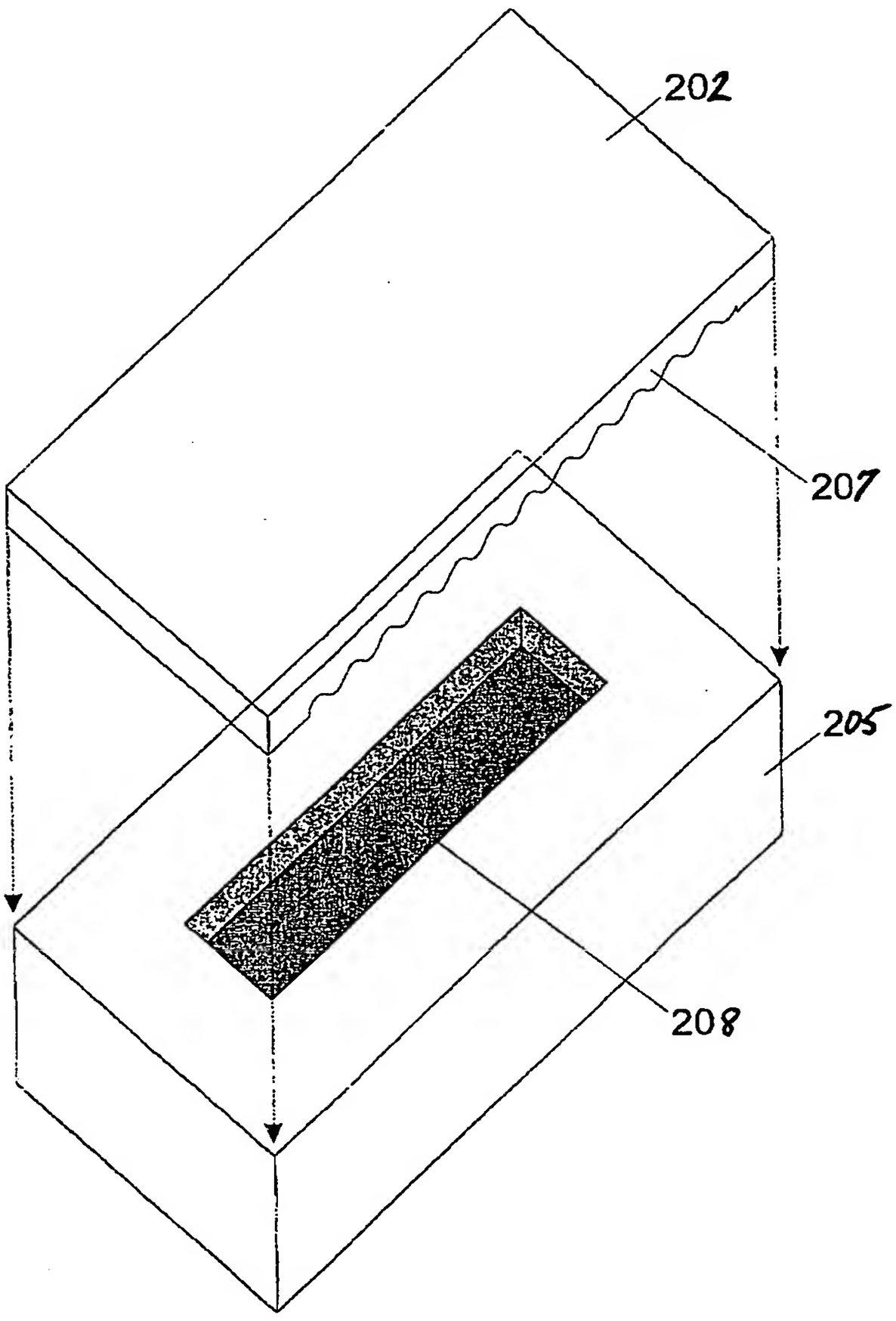
202
207
205
208

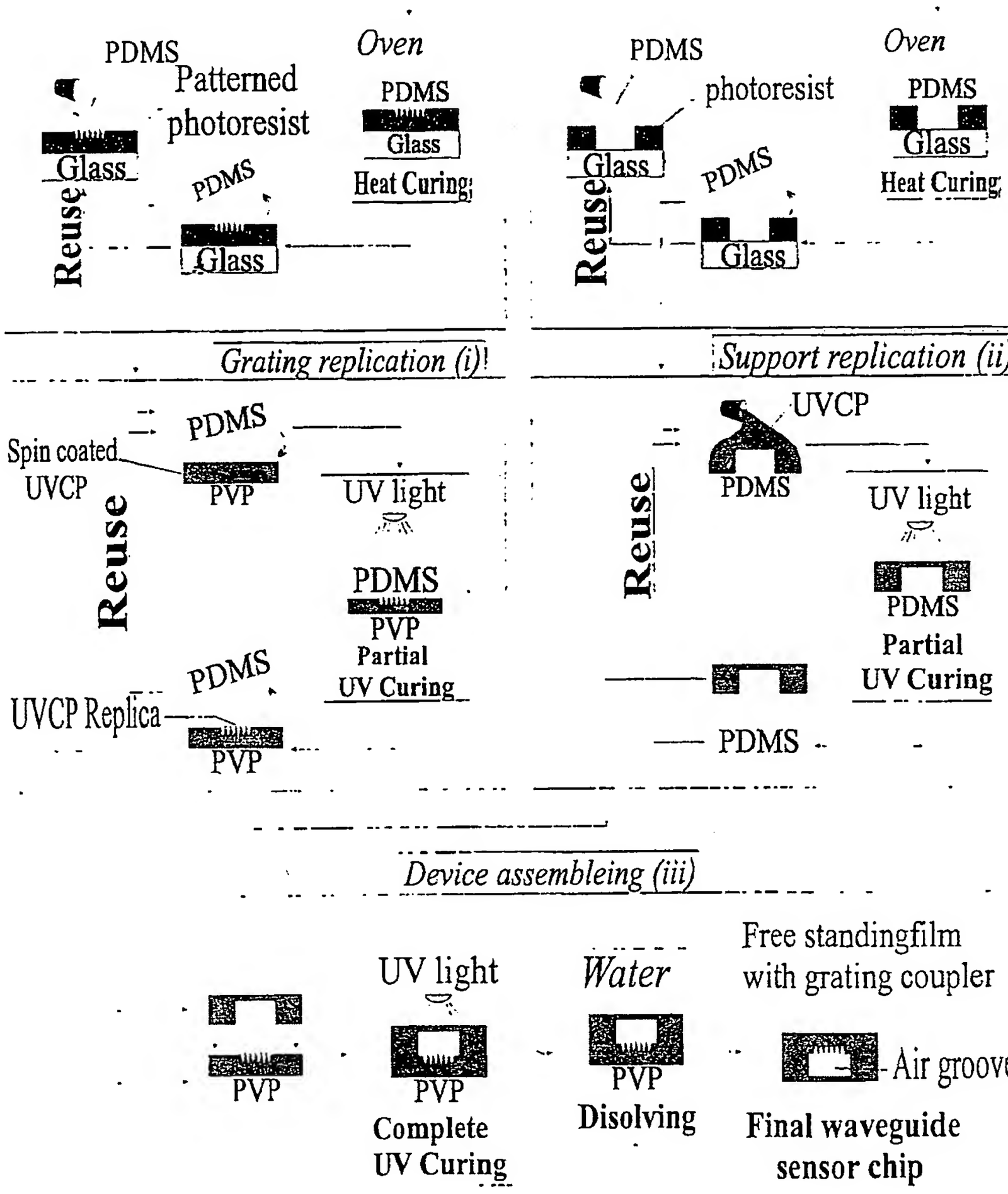
Grating stamp fabrication (i)
Support stamp fabrication (ii)
PDMS
Patterned photoresist
Glass
Reuse
PDMS
Glass
Oven
PDMS
Glass
Heat Curing
PDMS
photoresist
Glass
Reuse
PDMS
Glass
Oven
PDMS
Glass
Heat Curing
Grating replication (i)
Support replication (ii)
PDMS
Spin coated UVCP
PVP
Reuse
UV light
PDMS
PVP
Partial UV Curing
PDMS
UVCP Replica
PVP
UVCP
PDMS
Reuse
UV light
PDMS
Partial UV Curing
PDMS
Device assembleing (iii)
PVP
UV light
PVP
Complete UV Curing
Water
PVP
Disolving
Free standingfilm with grating coupler
Air groove
Final waveguide sensor chip

Figure 8

Fig. 9a

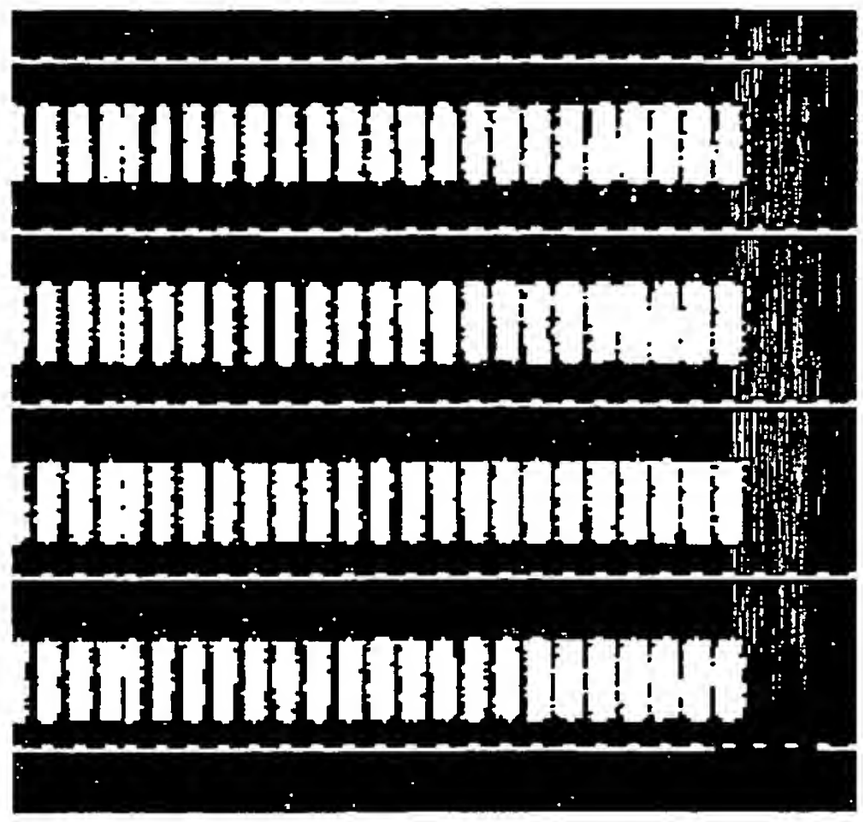

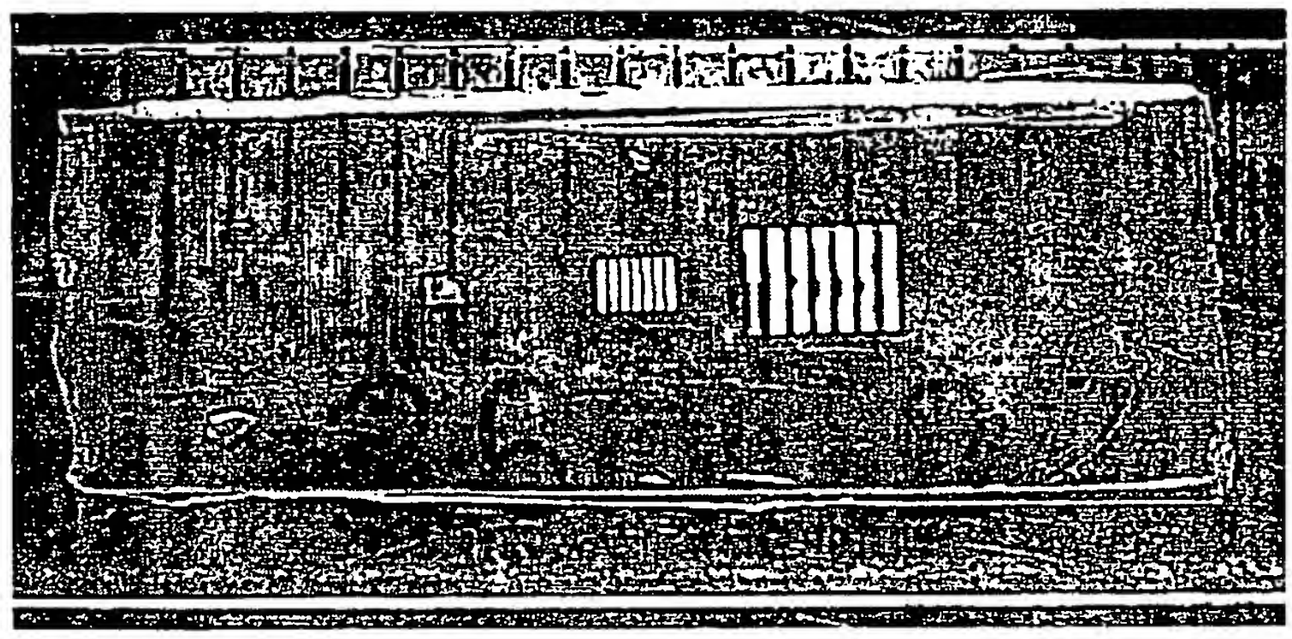

Fig 9b

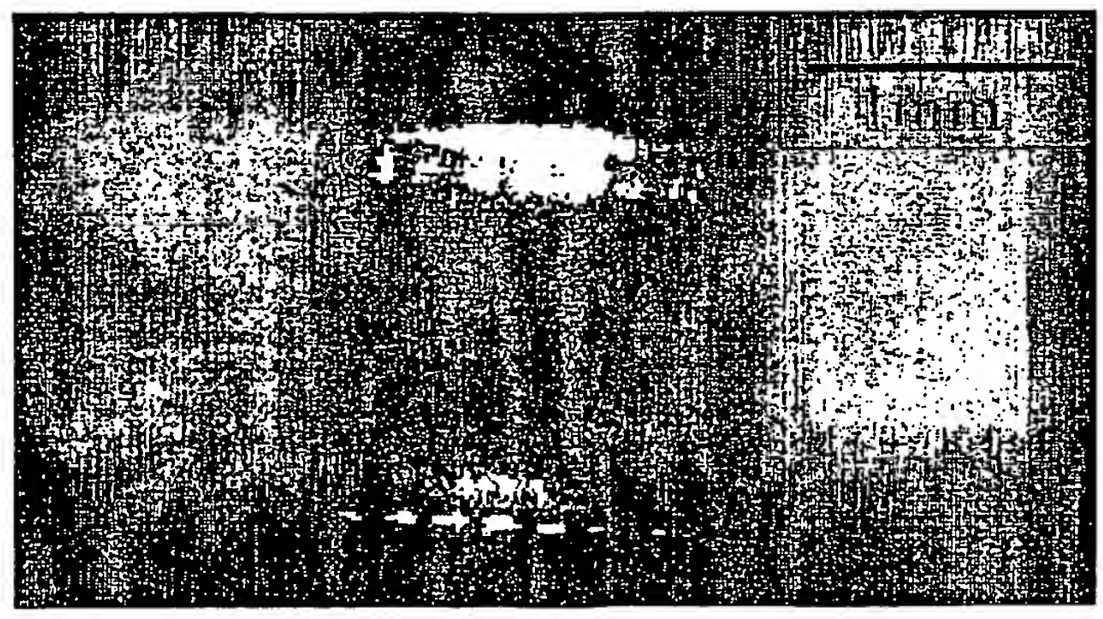

Fig. 10

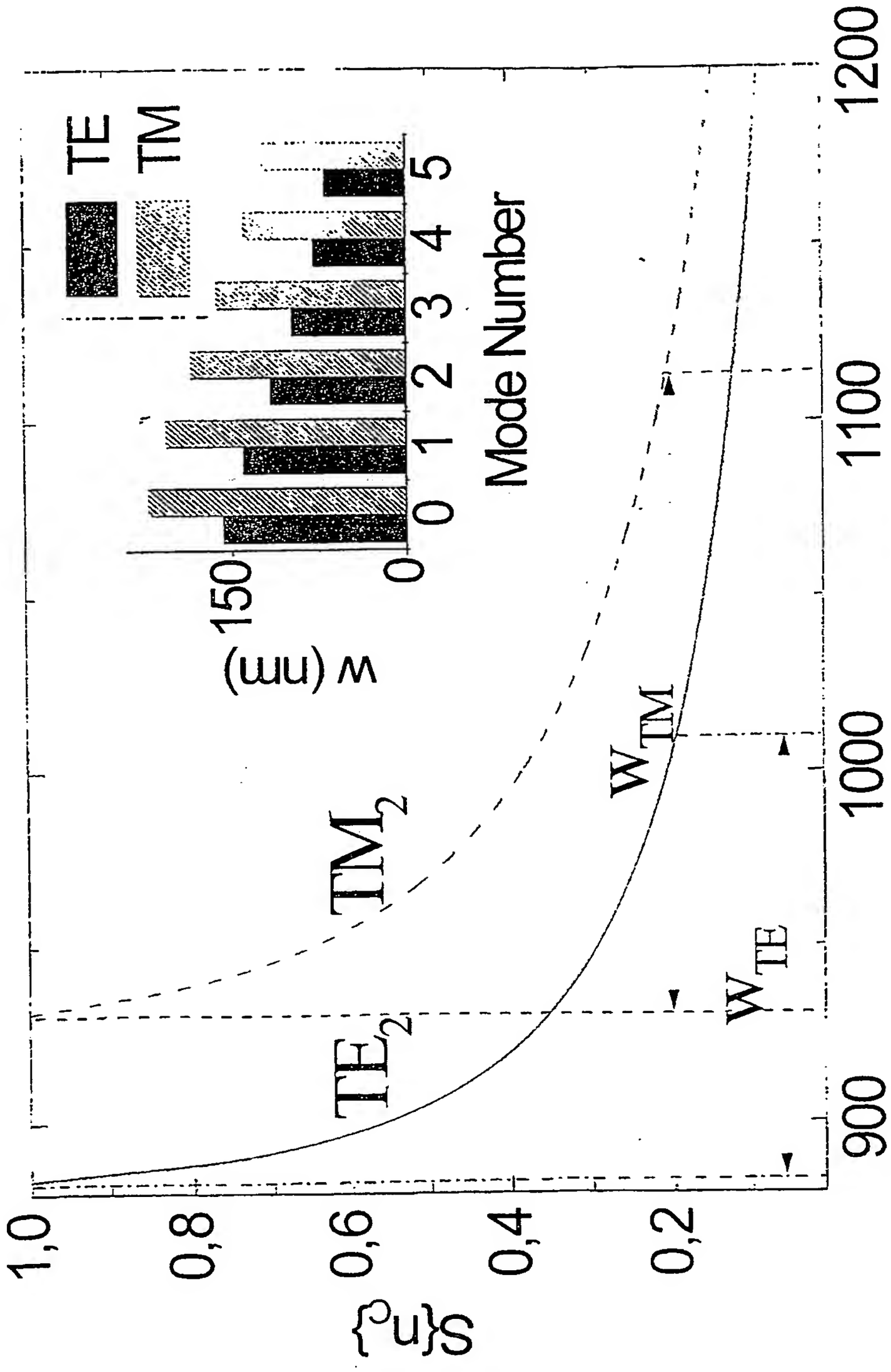
TE
TM
Mode Number
0 1 2 3 4 5
w (nm)
150
0
1200
1100
1000
900
d_F (nm)
TE_2
TM_2
W_{TM}
W_{TE}
1,0
0,8
0,6
0,4
0,2
{Pu}S

Fig. 11

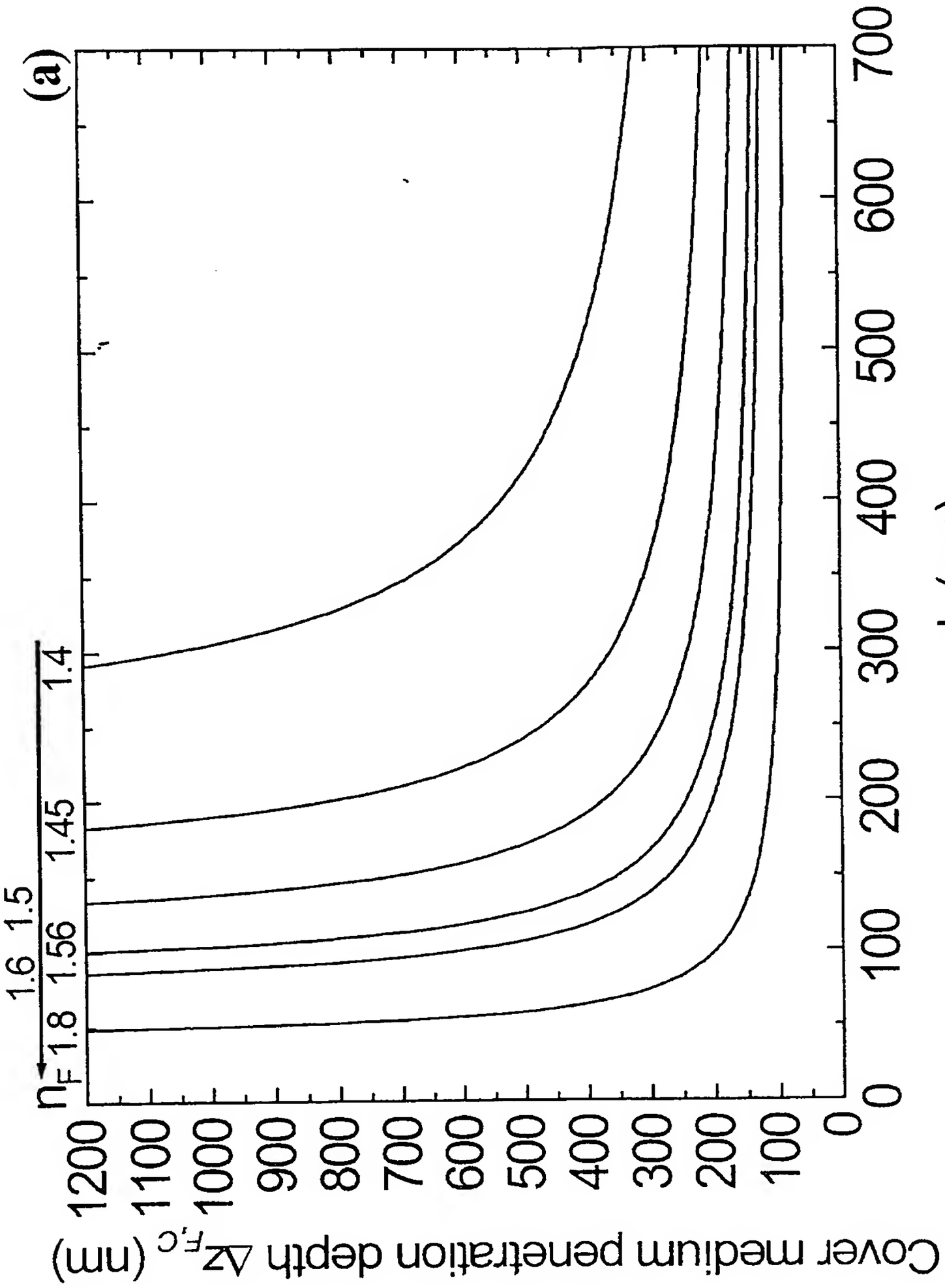
(a)
700
600
500
400
300
200
100
0
d_F (nm)
1.6 1.5
1.8 1.56 1.45 1.4
n_F
1200
1100
1000
900
800
700
600
500
400
300
200
100
0
Cover medium penetration depth $\Delta z_{F,C}$ (nm)

Fig. 12 a

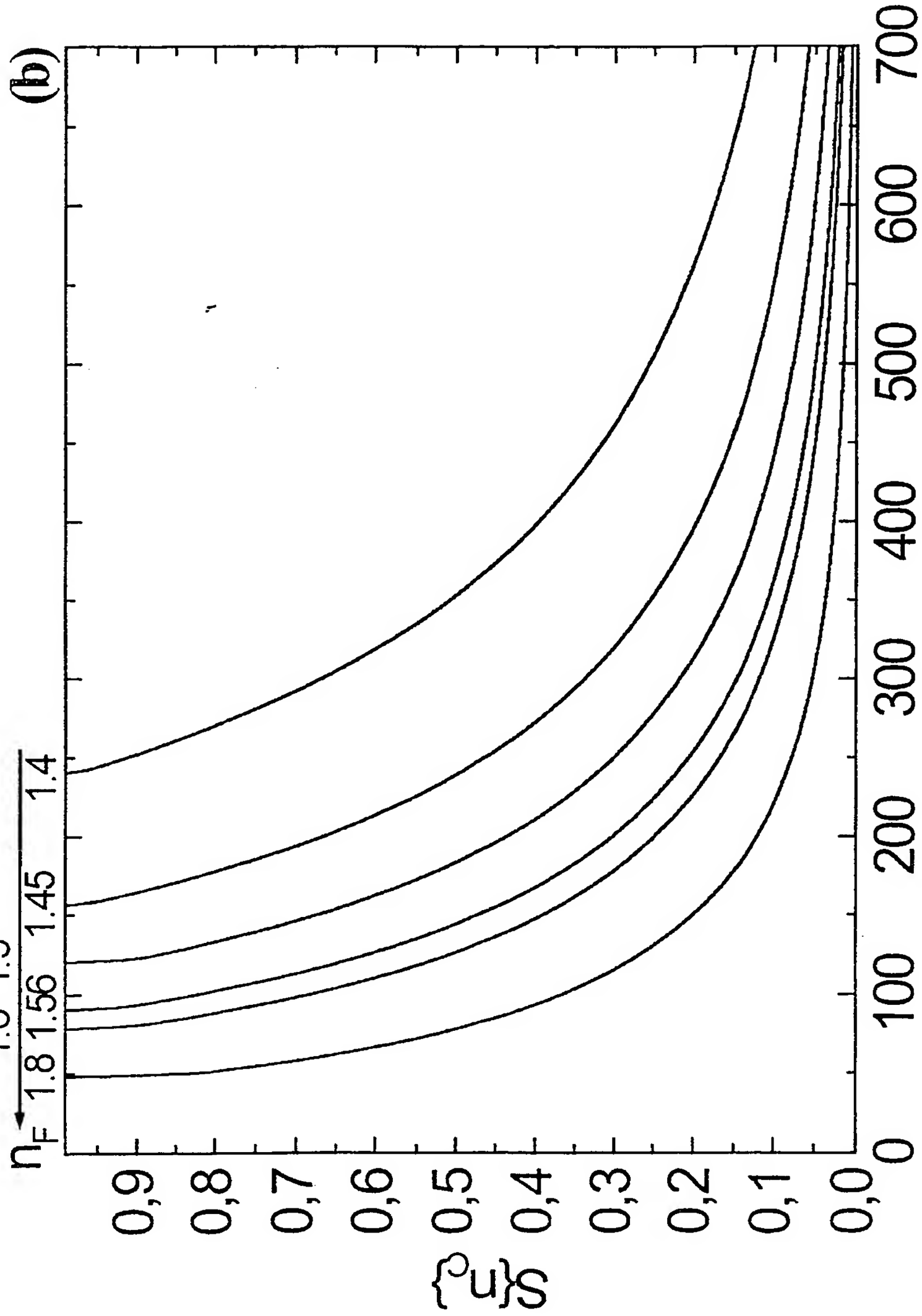
(b)
n_F
1.8
1.6
1.56
1.5
1.45
1.4
0,9
0,8
0,7
0,6
0,5
0,4
0,3
0,2
0,1
0,0
$\{^{\circ}u\}_S$
0
100
200
300
400
500
600
700
d_F (nm)

Fig 12b

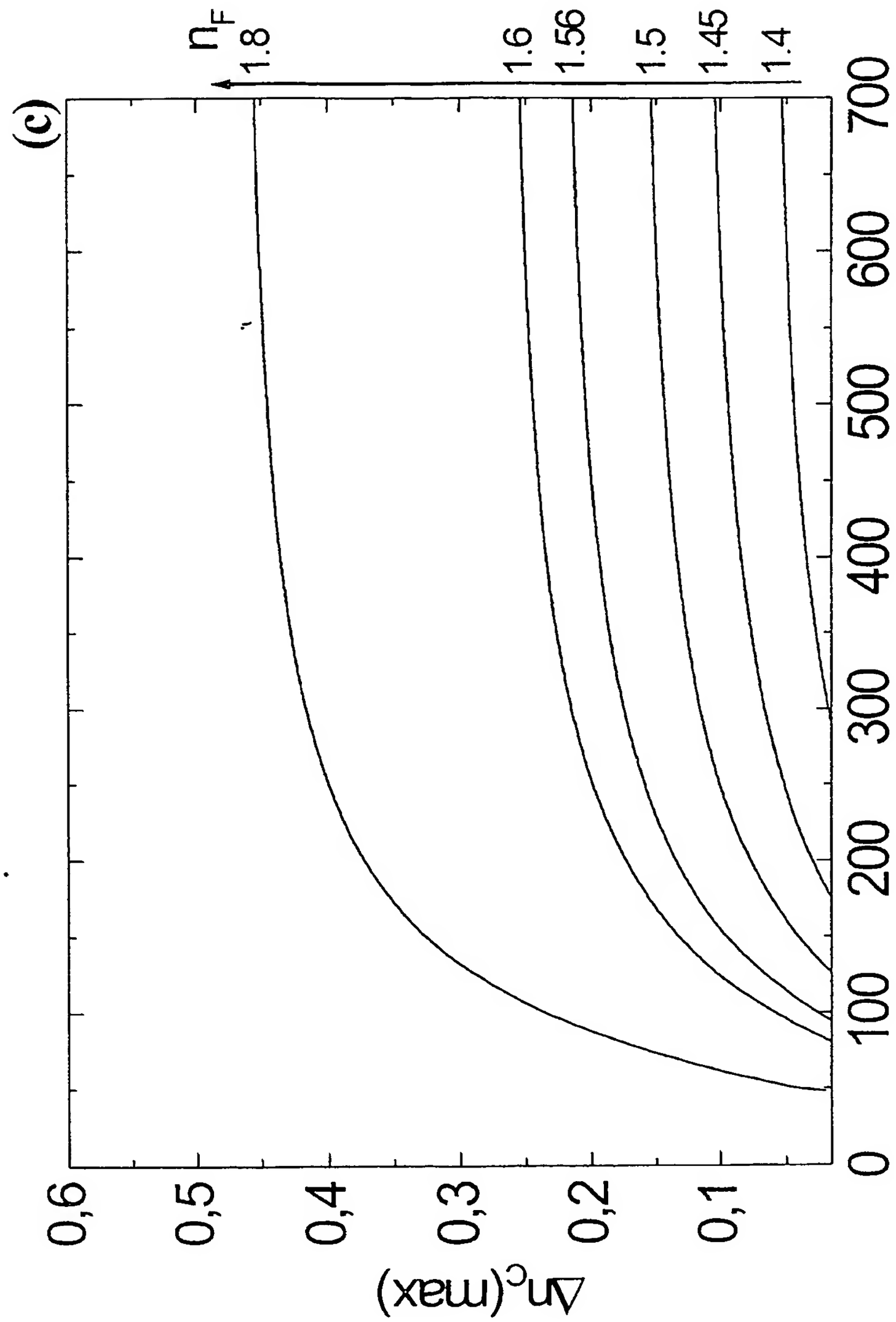
(c)
n_F
1.8
1.6
1.56
1.5
1.45
1.4
d_F (nm)
100
200
300
400
500
600
700
0
Δn_C(max)
0,6
0,5
0,4
0,3
0,2
0,1

Fig. 12 c

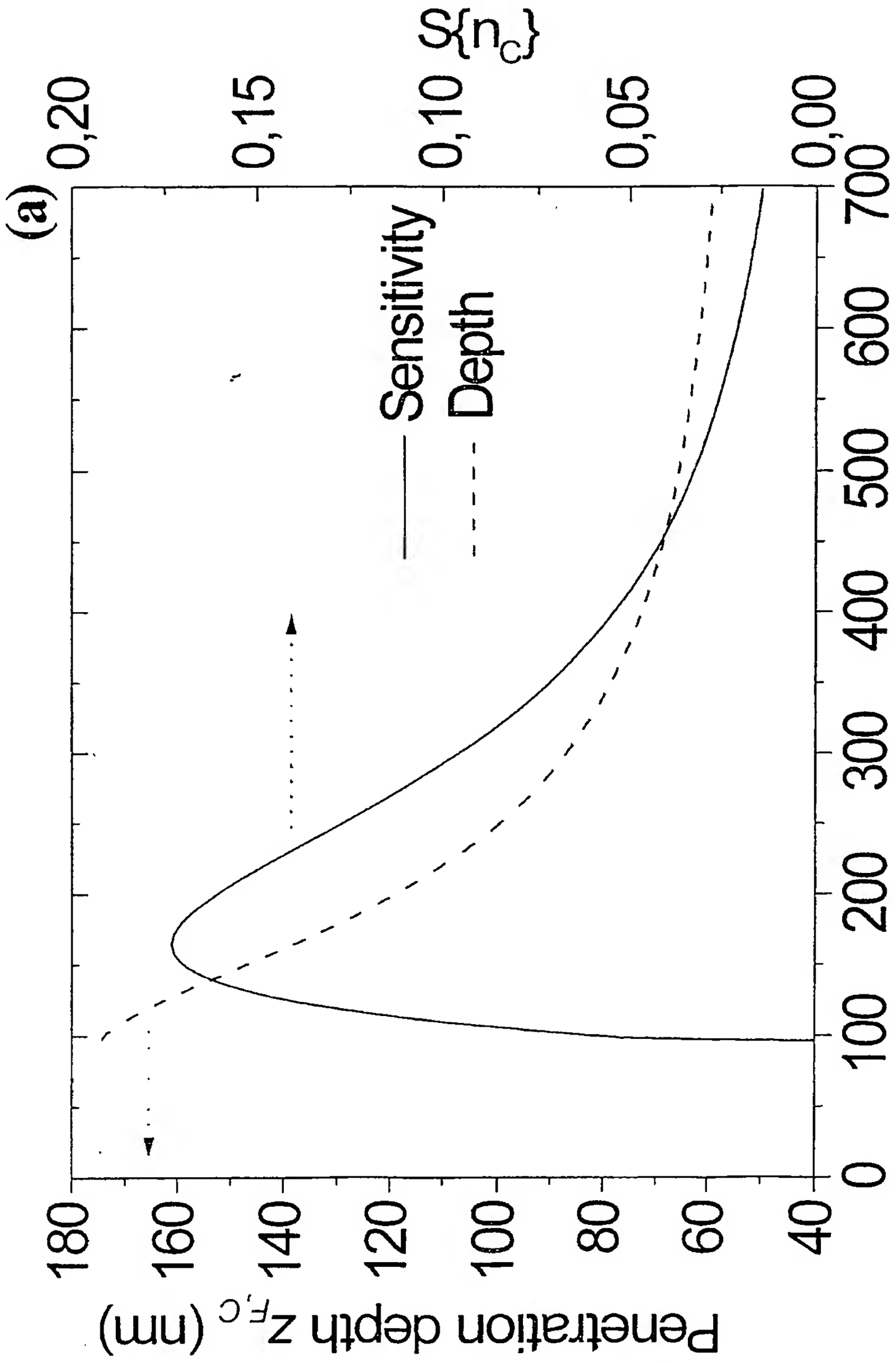
(a)
S{n_C}
0,20
0,15
0,10
0,05
0,00
Sensitivity
Depth
d_F (nm)
100
200
300
400
500
600
700
0
180
160
140
120
100
80
60
40
Penetration depth z_F,C (nm)

Fig. 13 a

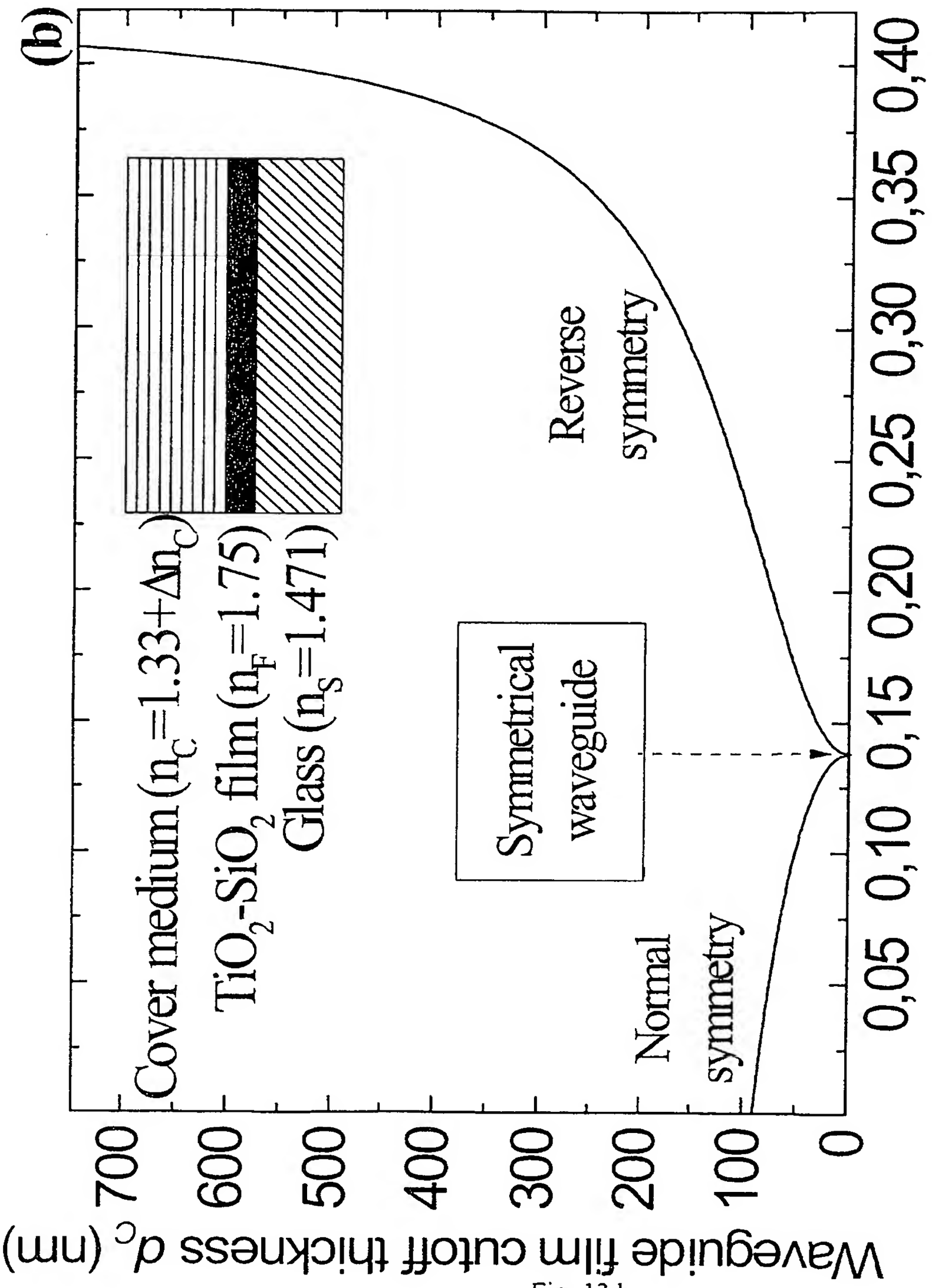
(b)
Cover medium (n_C=1.33+Δn_C)
TiO_2-SiO_2 film (n_F=1.75)
Glass (n_S=1.471)
Symmetrical waveguide
Reverse symmetry
Normal symmetry
Waveguide film cutoff thickness d_C (nm)
700
600
500
400
300
200
100
0
0,05
0,10
0,15
0,20
0,25
0,30
0,35
0,40
Δn_C

Fig. 13 b

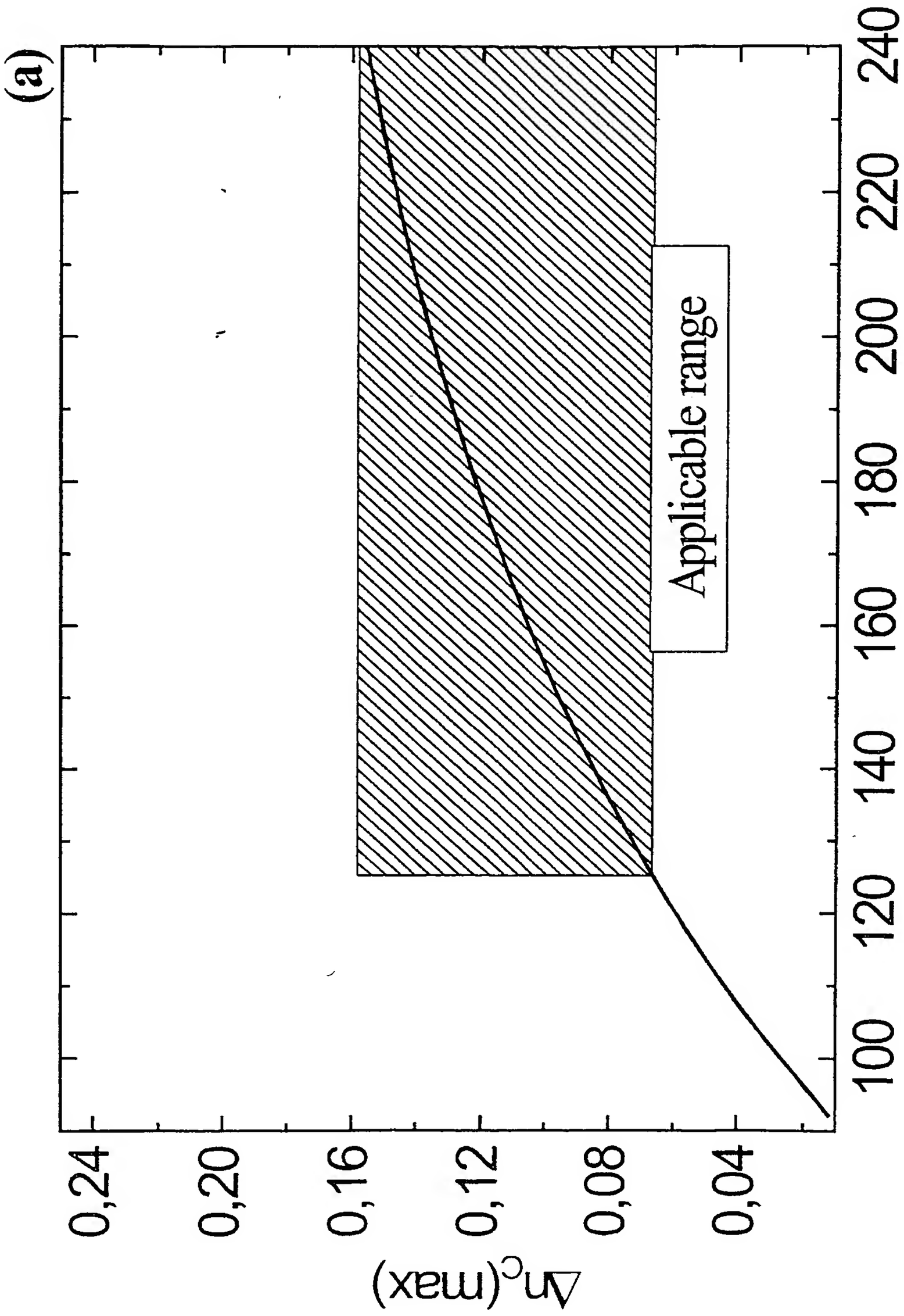
(a)
240
220
200
180
160
140
120
100
d_F (nm)
Applicable range
0,24
0,20
0,16
0,12
0,08
0,04
Δn_C(max)

Fig 14 a

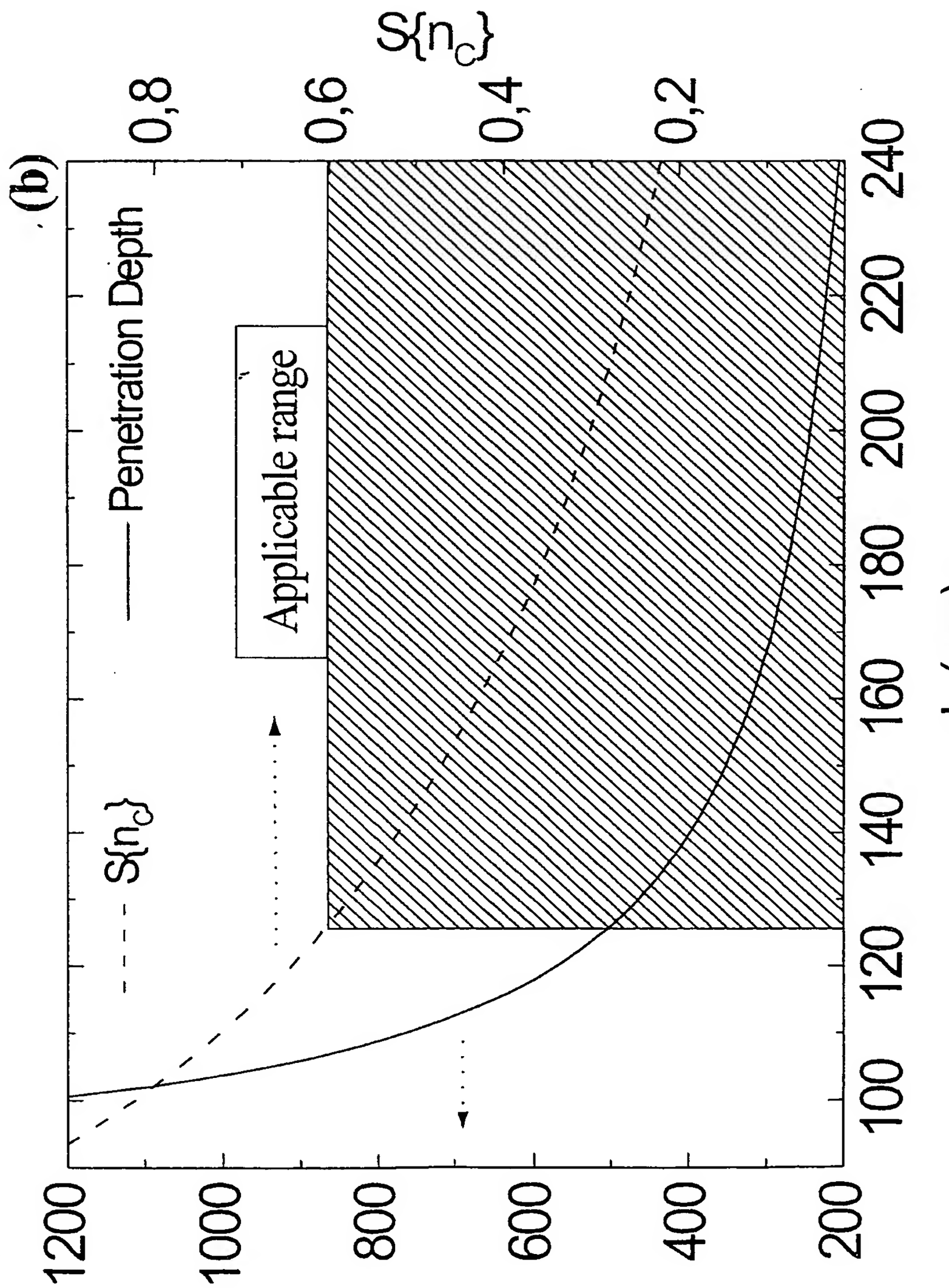
(b)
S{n_C}
0,8
0,6
0,4
0,2
240
220
200
180
160
140
120
100
Penetration Depth
S{n_C}
Applicable range
1200
1000
800
600
400
200
d_F (nm)
Cover medium penetration depth ΔZ_F,C (nm)

Fig 14 b

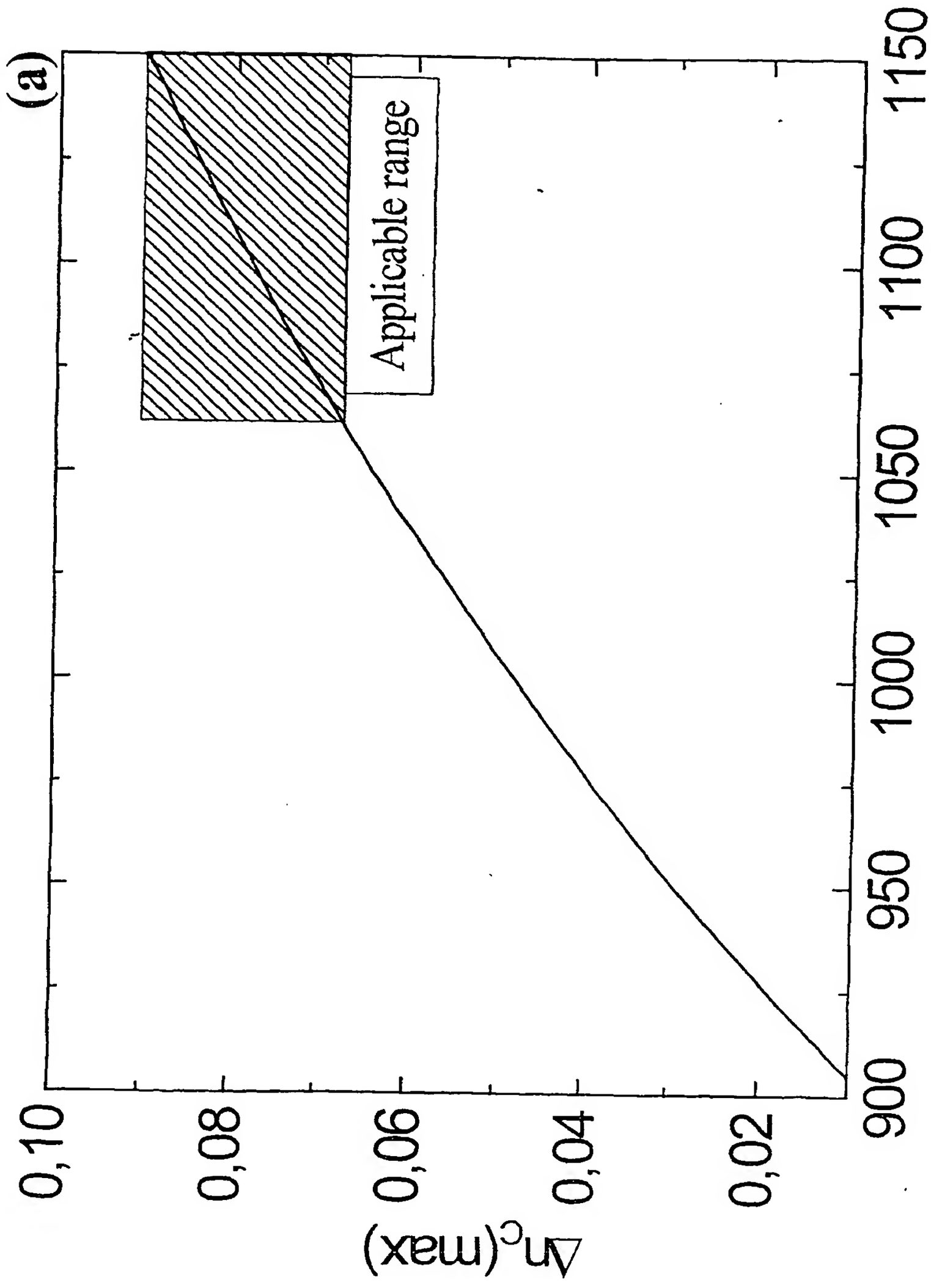
(a)
Applicable range
1150
1100
1050
1000
950
900
d_F (nm)
0,10
0,08
0,06
0,04
0,02
Δn_C(max)

Fig. 15 a

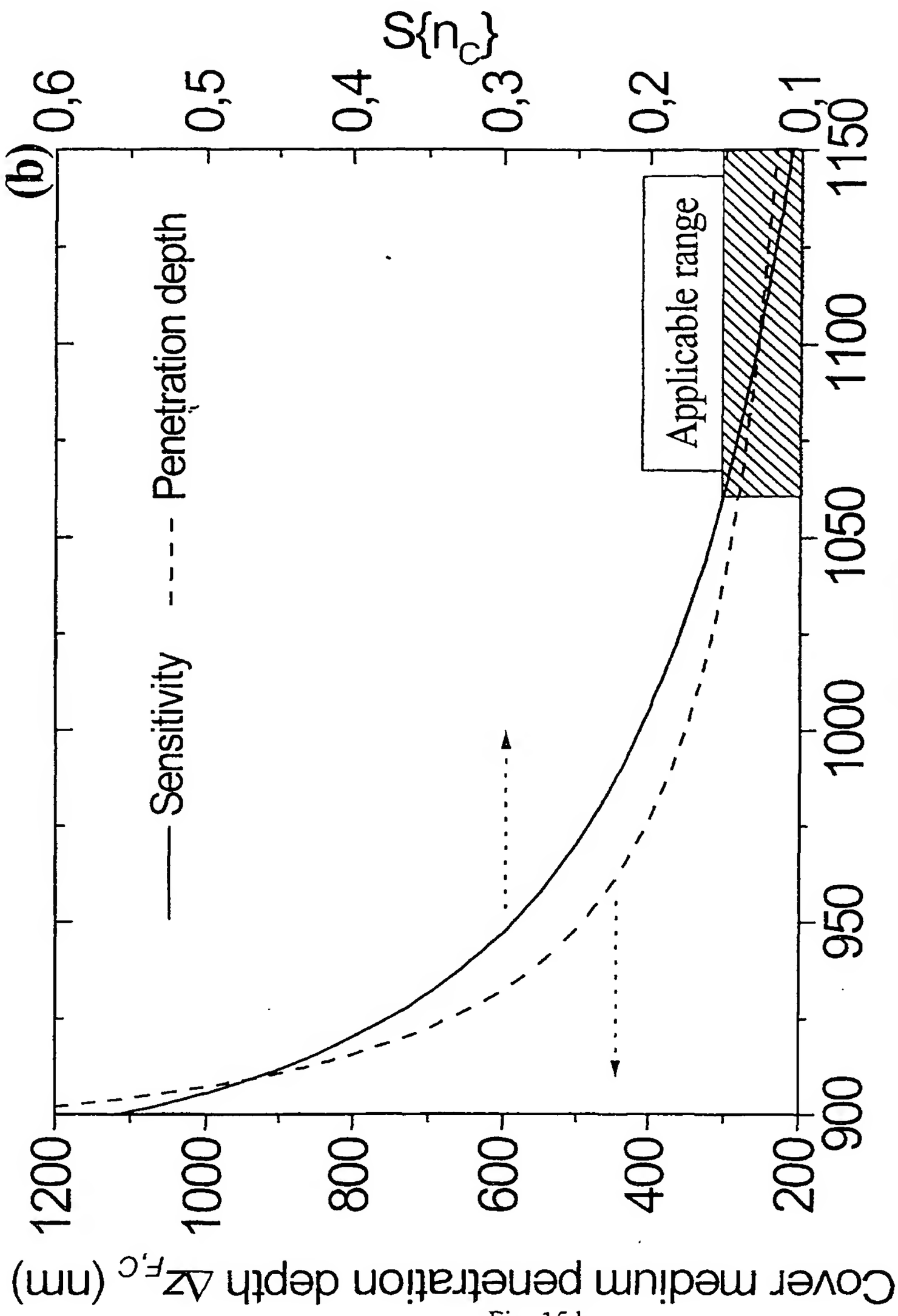
S{n_C}
0,6
0,5
0,4
0,3
0,2
0,1
(b)
Penetration depth
Sensitivity
Applicable range
1150
1100
1050
1000
950
900
d_F (nm)
1200
1000
800
600
400
200
Cover medium penetration depth ΔZ_F,C (nm)

Fig. 15 b

INTERNATIONAL SEARCH REPORT

	I nal Application No PCT/EP 01/12366

A. CLASSIFICATION OF SUBJECT MATTER
IPC 7 G01N21/77

According to International Patent Classification (IPC) or to both national classification and IPC

B. FIELDS SEARCHED

Minimum documentation searched (classification system followed by classification symbols)
IPC 7 G01N

Documentation searched other than minimum documentation to the extent that such documents are included in the fields searched

Electronic data base consulted during the international search (name of data base and, where practical, search terms used)
EPO-Internal

C. DOCUMENTS CONSIDERED TO BE RELEVANT

Category *	Citation of document, with indication, where appropriate, of the relevant passages	Relevant to claim No.
X	TIEFENTHALER K ET AL: "SENSITIVITY OF GRATING COUPLERS AS INTEGRATED-OPTICAL CHEMICAL SENSORS" JOURNAL OF THE OPTICAL SOCIETY OF AMERICA - B, OPTICAL SOCIETY OF AMERICA, WASHINGTON, US, vol. 6, no. 2, 1 February 1989 (1989-02-01), pages 209-220, XP000049843 ISSN: 0740-3224 cited in the application	1,3,9, 10, 14-20, 23,24
Y	page 213, right-hand column --- -/--	21,22

[X] Further documents are listed in the continuation of box C.

[ ] Patent family members are listed in annex.

* Special categories of cited documents :

"A" document defining the general state of the art which is not considered to be of particular relevance

"E" earlier document but published on or after the international filing date

"L" document which may throw doubts on priority claim(s) or which is cited to establish the publication date of another citation or other special reason (as specified)

"O" document referring to an oral disclosure, use, exhibition or other means

"P" document published prior to the international filing date but later than the priority date claimed

"T" later document published after the international filing date or priority date and not in conflict with the application but cited to understand the principle or theory underlying the invention

"X" document of particular relevance; the claimed invention cannot be considered novel or cannot be considered to involve an inventive step when the document is taken alone

"Y" document of particular relevance; the claimed invention cannot be considered to involve an inventive step when the document is combined with one or more other such documents, such combination being obvious to a person skilled in the art.

"&" document member of the same patent family

Date of the actual completion of the international search	Date of mailing of the international search report
21 February 2002	28/02/2002

Name and mailing address of the ISA	Authorized officer
European Patent Office, P.B. 5818 Patentlaan 2 NL - 2280 HV Rijswijk Tel. (+31-70) 340-2040, Tx. 31 651 epo nl, Fax: (+31-70) 340-3016	Tabellion, M

INTERNATIONAL SEARCH REPORT

In ional Application No
PCT/EP 01/12366

C.(Continuation) DOCUMENTS CONSIDERED TO BE RELEVANT

Category °	Citation of document, with indication,where appropriate, of the relevant passages	Relevant to claim No.
A	KUNZ R E: "Miniature integrated optical modules for chemical and biochemical sensing" SENSORS AND ACTUATORS B, ELSEVIER SEQUOIA S.A., LAUSANNE, CH, vol. 38, no. 1-3, 1997, pages 13-28, XP004083666 ISSN: 0925-4005 cited in the application	26
Y	page 20; figures 11,16-19 ---	21,22
A	LUKOSZ W: "Integrated optical chemical and direct biochemical sensors" SENSORS AND ACTUATORS B, ELSEVIER SEQUOIA S.A., LAUSANNE, CH, vol. 29, no. 1, 1 October 1995 (1995-10-01), pages 37-50, XP004000850 ISSN: 0925-4005 cited in the application -----	